AD_______________

Award Number: W81XWH-11-1-0061

TITLE: Role of Autophagy in Keratin Homeostasis in Breast Cancer

PRINCIPAL INVESTIGATOR: Sameera Kongara

CONTRACTING ORGANIZATION:
University of Medicine and Dentistry of New Jersey -Robert Wood Johnson Medical School
New Brunswick, NJ 08903.

REPORT DATE: December, 2012

TYPE OF REPORT: Annual Summary

PREPARED FOR: U.S. Army Medical Research and Materiel Command
Fort Detrick, Maryland 21702-5012

REPORT DOCUMENTATION PAGE

Form Approved OMB No. 0704-0188

1. REPORT DATE	2. REPORT TYPE	3. DATES COVERED
December2012	Annual Summary	1 December 2011–30 November 2012

4. TITLE AND SUBTITLE
Role of autophagy in keratin homeostasis in breast cancer

5a. CONTRACT NUMBER

5b. GRANT NUMBER
W81XWH-11-1-0061

5c. PROGRAM ELEMENT NUMBER

6. AUTHOR(S)
Sameera Kongara

E-Mail: kongarsa@umdnj.edu

5d. PROJECT NUMBER

5e. TASK NUMBER

5f. WORK UNIT NUMBER

7. PERFORMING ORGANIZATION NAME(S) AND ADDRESS(ES)

University of Medicine and Dentistry of New Jersey -Robert Wood Johnson
Medical School New Brunswick, NJ 08903.

8. PERFORMING ORGANIZATION REPORT NUMBER

9. SPONSORING / MONITORING AGENCY NAME(S) AND ADDRESS(ES)
U.S. Army Medical Research and Materiel Command
Fort Detrick, Maryland 21702-5012

10. SPONSOR/MONITOR'S ACRONYM(S)

11. SPONSOR/MONITOR'S REPORT NUMBER(S)

12. DISTRIBUTION / AVAILABILITY STATEMENT
Approved for Public Release; Distribution Unlimited

13. SUPPLEMENTARY NOTES

14. ABSTRACT
Autophagy is an evolutionarily conserved catabolic process where the proteins and organelles of a cell are degraded using the lysosome. Defective autophagy has been implicated in mammary tumorigenesis as autophagy deficient beclin1+/- mice develop mammary hyperplasias at a higher frequency than their wild-type counterparts and beclin1 is monoallelically deleted in 40% of human breast tumors. Phospho(S73)-K8, a modification required for keratin filament reorganization under stress, in autophagy-deficient cell lines, and mouse mammary tissues. We conclude that interfering with the phosphorylation of K8 at this residue however, does not appear to alter the reorganization of the keratin network under stress and therefore, are unable to investigate the role of this phosphorylation site in the context of autophagy deficiency. On the other hand, using gene expression analysis, we have identified increased Keratin 6 expression in autophagy-deficient cell lines, tumors generated from these cell lines and mouse mammary gland tissues. We are currently attempting to understand the association between of Keratin 6 expression and autophagy-deficiency in mammary tumorigenesis.

15. SUBJECT TERMS- Autophagy, Keratin 8, mammary tumorigeneis, Phospho(S73)-K8, Keratin 6

16. SECURITY CLASSIFICATION OF:			17. LIMITATION OF ABSTRACT	18. NUMBER OF PAGES	19a. NAME OF RESPONSIBLE PERSON USAMRMC
a. REPORT	b. ABSTRACT	c. THIS PAGE			19b. TELEPHONE NUMBER *(include area code)*
U	U	U	UU		

Table of Contents

Introduction:

Autophagy is an evolutionarily conserved process involving the targeting of cytoplasmic proteins and organelles to the lysosome via a double-membrane vesicle called the autophagosome. Defective autophagy has been implicated in mammary tumorigenesis as the essential autophagy gene, *beclin1*, is mono-allelically deleted in ~50% of breast tumors and *beclin1*$^{+/-}$ mice develop mammary hyperplasias. The increased tumorigenesis of autophagy-deficient cells is attributable to their propensity towards genomic instability. Our more recent work demonstrated that autophagy-deficient mammary cells have increased levels of ER and oxidative stress as well as abnormal keratin reorganization. Importantly, we identified increased levels of Phospho(S73)-K8, a modification that has previously been implicated in the reorganization of keratins, are associated with low Beclin1 levels in immortalized mouse mammary epithelial cells, tumors derived from these cells, and in native mouse mammary glands. Furthermore, high levels of Phospho(S73)-K8 were associated with low Beclin1 levels in human breast tumors, indicating that Phospho(S73)-K8 could potentially function as a marker for defective autophagy. In an attempt to generate a robust autophagy-deficiency signature that relied on a panel of proteins instead of a single marker, Phospho(S73)-K8, we began investigating potential differences in post-translational modifications on Keratin 8 and other members of the keratin family (as these are known to be heavily modified under stress) between autophagy-competent and deficient immortalized mammary epithelial cells; however, we were unable to detect any post-translationally modified keratin species that was unique to autophagy-deficient cells. Next, we investigated if interfering with Keratin 8 phosphorylation at Ser73 had a functional consequence on autophagy-competent and deficient cells with respect to their ability to survive under stress, and found no significant differences between the two cell lines. Therefore, phosphorylation of Keratin 8 at Ser73 appears to not have a significant effect on keratin network reorganization or the ability of cells to survive under stress. Next, we employed microarray analysis to investigate the differences between autophagy-competent and deficient cells and their ability to form tumors. One of the most highly upregulated genes in apoptosis-competent and disabled *beclin1*$^{+/-}$ cells was Keratin 6; in tumors derived from Bcl-2 overexpressing *beclin1*$^{+/-}$ cells, the degree of upregulation was even higher, indicating that high Keratin 6 expression might be a driver of tumorigenesis in an autophagy-deficient background. We are currently in the process of investigating the relationship between Keratin 6 and autophagy-deficiency and how it may play a role in driving tumorigenesis mediated by insufficient autophagy. Understanding the underlying mechanisms that are responsible for defective-autophagy driven tumorigenesis will aid in the development of successful treatment strategies of autophagy-competent and defective tumors.

Specific Aim 1: Identify the post-translational modifications, such as phosphorylation, glycosylation and ubiquitination, of keratin 8 and its obligate partner keratin 18 under normal, metabolic stress and recovery conditions in iMMECs in vitro.

Task 1: Identify post-translational modifications of keratins 8 and 18 in autophagy-competent (*beclin1*$^{+/+}$ and *atg 7*$^{+/+}$) and autophagy-deficient (*beclin1*$^{+/-}$ and *atg 7*$^{-/-}$) immortalized mouse mammary epithelial cells (iMMECs) under normal, metabolic stress (glucose and oxygen deprivation) and recovery conditions using mass spectrometry

Results:

<u>Year 1</u>

We first looked at the levels of keratin 8 and phopho(S73)-keratin 8 in apoptosis-inhibited *beclin1*$^{+/+}$ and *beclin1*$^{+/-}$ iMMECs overexpressing Bcl-2 under normal and metabolic stress (no glucose, low oxygen conditions mimicking the tumor microenvironment) conditions. Keratin 8 levels are modestly higher in the *beclin1*$^{+/-}$ cells compared to their wild-type counterparts (Figure 1A). The amount of phospho(S73)-keratin 8 in both *beclin1*$^{+/+}$ and *beclin1*$^{+/-}$ decreases with an increase in metabolic stress, and the protein levels increase during recovery (Figure 1A, D5+1dr), when cells are subjected to oxidative stress as normal oxygen and nutrient conditions are restored. The expression of phospho(S73)-keratin 8 has previously been reported as a marker of mitosis (Liao et al., 1997), apoptosis (Liao et al., 1997) and stress due to heat (Liao et al., 1997) and stimulation with Fas ligand (He et al., 2002). However, the expression of phopho(S73)-keratin 8 decreases in wild-type cells (by immunoblotting, Figure 1 and by immunofluorescence (Kongara et al., 2010)), while a conflicting picture emerges in *beclin1*$^{+/-}$ cells, with decreases detected by immunoblotting (Figure 1), and increases detected by immunofluorescence (Kongara et al., 2010).

Since phosphorylation of keratins is thought to play an important role in their solubility (Toivola et al., 2002), we examined the levels of K8 and phospho(S73)-K8 in the Triton-x soluble fraction and the insoluble fractions of protein extracts from *beclin1*$^{+/+}$ and *beclin1*$^{+/-}$ cells with Bcl-2. The level of K8, when examined by immunoblotting the high salt extract fraction, appears to be steady in the wild-type cells while more protein is detected upon the induction of stress in the heterozygous cells (Figure 1B, 1. K8). The level of keratin 8 does in fact, increase with metabolic stress since the protein from the cells metabolically stressed over days was collected in a fixed volume of lysis buffer, and there is a loss if viability of cells upon the induction of metabolic stress (Karantza-Wadsworth et al., 2007). Therefore, the presence of similar levels of protein from fewer cells indicates that the fraction of insoluble K8 increases in both the wild-type and heterozygous cells upon metabolic stress. Similarly, a Coomassie stained blot containing the insoluble proteins (equal volume lysate loaded from equal volume gels) detects equal amounts of K8 across the timepoints in the wild-type cells, and an increase in protein levels in the heterozygous cells (Figure 1D). Due to a loss of

viability of cells upon the induction of stress, the levels of insoluble keratin 8 increase in both the *beclin1*$^{+/+}$ and *beclin1*$^{+/-}$ cells overexpressing Bcl-2, given that the number of cells and protein concentration of equal volume lysates decreases over the stress period. Futhermore, the bands detected in the Coomassie gel are common to both *beclin1*$^{+/+}$ and *beclin1*$^{+/-}$ cells, with no unique band (migrating differences due to post-translational modifications such as phosphorylation or glycosylation) detected (Figure 1D). In the soluble fraction, K8 levels appear to be stable across the timepoints examined in both the *beclin1*$^{+/+}$ and *beclin1*$^{+/-}$ cells (Figure 1C). In the case of the soluble fraction, equal protein was loaded on the basis of the BCA-RAC protein quantitation assay; however, there is no direct means to verify equal loading. Proteins such as actin that are commonly used to verify loading in whole cell extracts are present in both the soluble and the insoluble fractions, thereby rendering them ineffective as controls for loading purposes.

Phospho(S73)-K8 is undetectable in the soluble fraction (Figure 1C), and levels of the protein in the insoluble fraction remain the same with upon metabolic stress, and increase slightly during recovery in the wild-type cells, while there appears to be a decrease in the levels of protein in the *beclin1*$^{+/-}$ cells upon induction of stress, and an increase during recovery (Figure 1B). However, there remains the difficulty of verifying the loading levels of protein, which has remained a persistent issue in our present pursuit. In general, a Coomassie stained gel containing the insoluble fraction is used as a loading control for immunoblotting various proteins from this fraction, while the cell number is normalized to study the protein levels in the soluble fraction. These controls are untenable in our case since we are interested in the differences between *beclin1*$^{+/+}$ and *beclin1*$^{+/-}$ cell lines as well as the differential effects of metabolic stress within each cell line. From the results presented thus far and our previous data (Kongara et al., 2010), it is evident that the levels of keratin 8 change upon the induction of stress and to different degrees between the wild-type and *beclin1*$^{+/-}$ cells, and therefore, the Coomassie stained gel would not be an ideal control to study proteins of the insoluble fraction by western blotting. Similarly, normalizing cell number as a means to control for loading for studying the proteins in the soluble fraction is not ideal for our purposes of comparing between autophagy-competent and impaired cell lines, since autophagy is critical for protein turnover, and could directly affect overall protein content and therefore, levels of protein. Problems with controlling protein loading also make performing an immunoprecipitation of keratins challenging, since keratins are fairly insoluble proteins, and the detergents that have a higher efficiency solubilizing keratins such as Empigen BB successfully dissolve only around 50% of the total keratin pool (Ku et al., 2004), and therefore, quantifying any observed differences between autophagy-competent and deficient cells can be arduous.

Phosphorylation of Keratin 8 at Serine-73 has previously been reported to be important for keratin filament reorganization (Ku et al., 2002). Upon treatment with okadaic acid, a majority NIH-3T3 cells transfected with K8 S73A (point mutation at position 73, resulting in an alanine substitution for a serine residue) construct had intact filaments while cells with WT K8 and K8 S73D (a phosphorylation mimicking construct) had significant reorganization; no difference in filament organization was observed using all three constructs under regular growth conditions (Ku et al, 2002). Since

phosphorylation of keratin 8 is modulated under stress (Ku et al., 2002), and *beclin1*$^{+/+}$ and *beclin1*$^{+/-}$ cells behave differentially under stress (Karantza-Wadsworth et al., 2007, Kongara et al., 2010), we examined whether the differences manifest between cells of the two genotypes were modulated by Keratin 8 phosphorylation at serine 73. Towards this end, we stably transfected iMMECs of both genotypes with WT K8, K8 S73A and K8 S73D constructs, and examined the effects of metabolic stress upon viability and filament reorganization using clones expressing comparable levels of protein (Figure 2A). In both *beclin1*$^{+/+}$ and *beclin1*$^{+/-}$ cells, the S73D mutant survived better than the S73A or the WT construct (Figure 2B). However, there were no discernable differences in the filament organization upon the induction of stress in cells overexpressing WT K8, K8 S73A or K8 S73D, irrespective of the genotype (TROMA-1/K8 staining, Figure 3). While the levels of Phospho(S73)-K8 increase more in the *beclin1*$^{+/-}$ cells compared to the *beclin1*$^{+/+}$ cells upon the induction of stress, consistent with previous results (Kongara et al., 2010), there was no observable difference between the WT K8, K8 S73A and K8 S73D within each genotype (Figure 4), indicating that the overexpression of wild-type or mutant constructs does not interfere with phosphorylation (Figure 4) or reorganization of the keratin network (Figure 3). Furthermore, we tested whether two parental clones of *beclin1*$^{+/+}$ and *beclin1*$^{+/-}$ cells overexpressing WT K8, K8 S73A and K8 S73D would differ in their ability to handle stress caused by treatment with Hanks buffered salt solution (HBSS), which results in amino acid deprivation. Our viability assays in HBSS do not result in the emergence of a consistent trend among the two *beclin1*$^{+/+}$ and *beclin1*$^{+/-}$ clones, with the K8 S73A overexpressing cell line being the best survivor in one wild-type parental (Clone 1), while the WT K8 survives best in the other parental cell line of the same genotype (Clone 2); in the *beclin1*$^{+/-}$ cells, the S73D mutant survives best in the parental Clone 1 while it does poorly in the Clone 2 (Figure 5). Hence, there is clonal variability, and no consistent trend emerges. Taken together, phosphorylation of Keratin 8 at serine 73 does not appear to be important for the survival differences observed in *beclin1*$^{+/+}$ and *beclin1*$^{+/-}$ cells under stress (Figure 2B and 5), or keratin filament reorganization under stress (Figure 3 and 4).

Recently, we analyzed *beclin1*$^{+/+}$ and *beclin1*$^{+/-}$ iMMECs with and without the overexpression of Bcl-2 as well as tumors generated from orthotopic implantation of Bcl-2 overexpressing iMMECs in immuno-compromised mice, by using gene expression profiling. One of the most upregulated genes in autophagy compromised cells and tumors in our study was keratin 6, which was expressed over 8-fold and 10-fold in *beclin1*$^{+/-}$ iMMECs without and with Bcl-2 respectively, compared to their wild-type counterparts (Figure 6). Tumors generated from autophagy compromised iMMECs overexpressing Bcl-2 exhibited an even greater upregulation of keratin 6 with *beclin1*$^{+/-}$, Bcl-2 tumors expressing over 35-fold higher levels of keratin 6 mRNA compared to their wild-type counterparts (Figure 6). Furthermore, we examined mammary glands from both virgin and multiparous, 11 month old *beclin1*$^{+/+}$ and *beclin1*$^{+/-}$ mice, and observed the presence of distinct Keratin 6 cells in *beclin1*$^{+/-}$ glands irrespective of the pregnancy status, while the wild-type gland had few Keratin 6 positive cells (Figure 7). In the developing and proliferating mammary glands from 4.5-week old mice, Keratin 6 expression is higher in *beclin1*$^{+/-}$ tissue compared to *beclin1*$^{+/+}$ tissue (Figure 8). Although the precise function of Keratin 6 is unknown, it is sporadically expressed in the

terminal end buds of developing mammary glands (Smith et al., 1990, Sapino et al., 1993), and has more recently been reported as a marker of bipotent progenitor cells (Bu et al., 2011). Mice that develop mammary tumors due to the presence of transgenic Wnt1 or other downstream components of this pathway, including β-catenin and c-myc, have an increased population of K6 cells (Li et al., 2003). Additionally, in the skin, Keratin 6 expression is necessary for a rapid wound healing response (Wojcik et al., 2000). Given that Keratin 6 expression is associated with autophagy-deficiency, we are interested in understanding the basis for this association and if Keratin 6 expression is linked to the tumor initiating potential of autophagy-impaired cells. Towards this end, we will be generating *beclin1*$^{+/+}$ and *beclin1*$^{+/-}$ iMMECs overexpressing Bcl-2 with a stable knockdown of keratin 6, and examining their ability to tolerate metabolic stress as well as their tumor forming capabilities.

<u>Year 2</u>

Results:

We obtained a set of GFP-tagged short hairpin RNAs targeting K6 and transiently expressed the vectors in *beclin1*$^{+/+}$ and *beclin1*$^{+/-}$ iMMECs overexpressing Bcl-2 to determine which hairpins were most efficient in reducing the levels of Keratin 6. As shown if Figure 9, shRNA #2 and shRNA #3 were most the most effective in knocking down K6 levels. Next, we generated stable clones of *beclin1*$^{+/+}$ and *beclin1*+/- iMMECs that expressed the GFP-tagged K6 shRNA (#2 and #3) or a non-targeting/luciferase-targeting vector as controls. Upon the examination of these clones, we observed that some *beclin1*$^{+/-}$ clones expressing the control hairpins had little to no K6 protein (Figure 10). This result indicated that the K6 expression within the *beclin1*$^{+/-}$ cell line might be variable. Therefore, we examined the levels of Keratin 6 by immunofluorescence in *beclin1*$^{+/+}$ and *beclin1*$^{+/-}$ cells. As shown in Figure 11, consistent with our gene expression analysis results, *beclin1*$^{+/-}$ cells express more K6 than *beclin1*$^{+/+}$ cells; however, the expression is heterogenous as only a some cells in a given population are K6. Next, we examined tumors derived from *beclin1*$^{+/+}$ and *beclin1*$^{+/-}$ overexpressing Bcl-2 iMMECs for their K6 expression and observed that while autophagy-deficient tumors had higher levels of K6, only a subset of cells within the tumor expressed K6 (Figure 12). Furthermore, examination of human breast cancer cell lines HCC1937 and HCC1954, which have low Beclin1 levels in a panel of human breast cancer cell lines, also revealed the presence of a few distinct K6 positive cells (Figure 13). Finally, K6 expression has been reported to be both constitutive and inducible in the skin, although there are currently no reports on whether its expression in the mammary gland is constitutive or inducible. Taken together, these observations indicate that knocking down the expression of an inducible protein such as K6 is not a feasible task.

Since K6 expression is most evident in developing mammary and we observe differences in K6 expression of *beclin1*$^{+/+}$ and *beclin1*$^{+/-}$ glands, we examined whole mounts of mammary glands from 6.5-week old *beclin1*$^{+/+}$ and *beclin1*$^{+/-}$ mice to look for differences in post-natal mammary gland development. As shown in Figure 14,

mammary glands from *beclin1*$^{+/-}$ mice exhibited increased side-branching and more ductal filling compared to *beclin1*$^{+/+}$ mice. The mammary gland is a unique organ in the fact that most of its development occurs post-natally. At birth, the mammary epithelium consists of a rudimentary ductal structure that is confined to the nipple area, which during puberty, elongates and branches to occupy the fat pad of the mammary gland. Subsequent estrus cycles regulate side-branching, which refers to the outgrowth of small epithelial structures from the primary ducts. Pregnancy increases side-branching and promotes the formation of alveoli, which are the structures responsible for the production of milk. Upon the weaning of pups, involution commences where the mammary gland reverts to its pre-pregnant state (Brisken and O'Malley, 2010).

Pubertal mouse mammary gland development, which begins at 3 weeks and continues up to 8 weeks of age, is regulated by the confluence of systemic hormones including estrogen, progesterone and prolactin and local growth factors such as Insulin growth factor-1 (IGF-1), Hepatocyte growth factor (HGF), and Fibroblast growth factor (FGF) (Parmar and Cunha, 2004, Stingl, 2011). Estrogen initiates pubertal ductal outgrowth and branching, while progesterone influences the side branching of the duct during the estrus cycle in a paracrine manner via the progesterone receptor (PR), RANKL and Wnt4 (Stingl, 2011). It is thought that under the influence of estrogen, ER^+ epithelial cells release the membrane protein Amphiregulin in a manner dependent upon its cleavage by the protease ADAM17 (Brisken and O'Malley, 2010). Following its release, Amphiregulin binds to EGFR present in the stroma. Additional factors released by the stroma that are yet to be identified are believed to cause the proliferation of the epithelial cells (Brisken and O'Malley, 2010). Thus, extensive crosstalk between the epithelium and the stroma via paracrine signaling is responsible for the proliferation and normal development of the mammary gland. In keeping with the theme of paracrine signaling in normal mammary gland development, PR^+ cells secrete RANKL upon the induction of progesterone. This secreted RANKL elicits a proliferative response in PR^- cells via the action of Wnt4 although the precise details of this process are unknown (Brisken and O'Malley, 2010).

To test if increased PR and RANKL signaling is responsible for the increased side branching observed, we stained mammary gland tissues from 5 and 6.5-week old *beclin1*$^{+/+}$ and *beclin1*$^{+/-}$ mice for these proteins together with the proliferation marker, Ki67. Indeed, higher levels of Ki67, PR and RANKL signaling are observed in the *beclin1*$^{+/-}$ glands (Figures 15-19), indicating that the increased proliferation observed in *beclin1*$^{+/-}$ glands maybe due to increased PR and RANKL signaling. Recent work from other laboratories has demonstrated that MMTV-RANKL transgenic mice have extensive side-branching and develop hyperplasia but not tumors in the mammary gland, in a manner strikingly similar to *beclin1*$^{+/-}$ mice (Fernandez-Valdivia et al., 2009). Importantly, RANKL mice have been reported to be susceptible to 7,12-dimethylbenz[a]anthracene (DMBA)-induced carcinogenesis in the presence of progesterones (Gonzalez-Suarez et al., 2010). Furthermore, it has been demonstrated that the mammary stem cell compartment expansion in response to progesterone is mediated by RANKL, and the absence of RANKL delays hormone-induced tumorigenesis (Schramek et al., 2010). Since we detect increased side-branching, PR and RANKL

signaling, we hypothesize that the tumorigenic potential of *beclin1*$^{+/-}$ mice is mediated by RANKL and its associated signaling pathway, thereby increasing the susceptibility of these mice to DMBA-induced tumorigenesis. We are currently in the process of testing this hypothesis.

Interestingly, increased RANKL staining is observed in the epithelial cells in 6.5-week old glands (Figure 19), while RANKL appears to be localized to the stroma (Figure 17), which consists of fibroblasts, adipocytes, and immune cells, in the *beclin1*$^{+/-}$ glands at 5 weeks, indicating that the autophagy-deficiency in the stromal compartment could be responsible for the increased side-branching observed in *beclin1*$^{+/-}$ glands. Of note, autophagy-defective macrophages have been demonstrated to have aberrant cytokine secretion due to increased inflammasome activity. Inflammasomes are protein complexes that function to process pro-caspase-1 into its active form (Martinon et al., 2009). Following activation, caspase-1 in turn processes cytokines such as IL-1β and IL-18, leading to their maturation and secretion. Importantly, the NLRP3 inflammasome, which is present in immune cells, is activated in response to a wide variety of stimuli including ROS and impaired phagocytosis (Martinon et al., 2009, Gross et al., 2011). Additionally, autophagy-impaired (Atg7$^{-/-}$, Atg16L$^{-/-}$, LC3$^{-/-}$ and Beclin1$^{+/-}$) macrophages secrete high levels of IL-1β and IL-18 due to increased inflammasome activity; this increased activity is triggered by the high levels of ROS detected in autophagy-defective macrophages (Saitoh et al., 2008, Nakahira et al., 2011, Zhou et al., 2011). While these two cytokines themselves have not been implicated in mammary gland development as yet, we hypothesize that aberrant cytokine secretion by autophagy-deficient immune cells could result in increased proliferation in the mouse mammary gland leading to increased tumorigenesis. In support of this possibility, we observe elevated levels of TNF-α and IL-1β in the stroma of 5-week old *beclin1*$^{+/-}$ mammary glands (Figure 20 and 21). To test if increased oxidative stress is responsible for the increased levels of cytokines, proliferation and tumorigenic potential of the autophagy-deficient *beclin1*$^{+/-}$ glands, we plan to treat mice with the anti-oxidant, N-Acetyl Cysteine and monitor the development of the mammary gland.

Specific Aim 3: Determine beclin1 levels, expression of other essential autophagy regulators, such as LC3, atg5 and atg7, and levels of post-translationally modified keratins 8 and 18 and their interactors in human breast cancer specimens to identify potential autophagy functional status signatures in breast cancer.

Task 1: Human breast cancer tumor microarrays will be obtained from Yale Cancer Center Tissue Microarray Facility (in collaboration with Dr. Bruce Haffty, CINJ) and stained using immunohistochemistry for autophagy regulators such as beclin1, LC3, atg5 and atg7 together with keratins 8, 18 and their post-translational modifications identified in Aim1, as well as proteins found to be important for keratin remodeling in Aim2. Staining patterns will be scored by two independent investigators, and will hopefully result in the generation of signatures for the functional status of autophagy in breast tumors. (1 year)

Results:

<u>Year 1:</u>

In collaboration with Dr. Bruce Haffty, we stained a tumor microarray containing 516 tissue specimens from patients whose medical history including hormone receptor and metastases status was known with antibodies recognizing the Phospho(S73)-K8 epitope, and scored them based on a scale from 0 to 3 where 0 corresponds to little to no staining, while 3 denotes very high levels of protein expression. Statistical analysis in collaboration with Dr. Dirk Moore, revealed the association of high levels Phospho(S73)-K8 with low levels of distant metastasis ($p<0.05$). Additionally, we stained another TMA obtained from NCI that had accompanying patient case history with the same antibody, and scored them on a scale of 0 to 4, with 0 representing the detection of no protein and 4 the highest levels. As shown in Figure 9, 41.8%, 60.9% and 49% of invasive node negative, node positive and distant metastases samples respectively, stained for no Phospho(S73)-K8 (0 staining), while few samples of normal breast tissue (24.3) and normal breast-fibroadenoma (28.2%) demonstrated this phenomenon. Since high Beclin1 levels correlate with low Phospho(S73)-K8 levels (Kongara et al., 2010), which in turn appears to correlate with invasive potential, we are interested in pursuing if autophagy status impacts progression to metastases.

<u>Year 2:</u>

We are in the process of staining a tumor microarray to correlate the levels of Keratin 6 with autophagy deficiency status, by staining it for the levels of Beclin1.

Key Research Accomplishments:

<u>Year 1:</u>

- Identifying the association between low levels of Phospho(S73)-K8 with high levels of distant metastasis.
- Identifying increased K6 (a marker of bipotent progenitor cells) mRNA levels in autophagy-deficient cell lines, tumors generated from these cell lines and mouse mammary gland tissues compared to their wild-type counterparts.
- Identifying that overexpression of WT and mutant keratin constructs does not disrupt the keratin network in *beclin1*$^{+/+}$ and *beclin1*$^{+/-}$ iMMECs under conditions of metabolic stress; additionally, overexpression of WT or mutant keratin constructs does not impact viability of *beclin1*$^{+/+}$ and *beclin1*$^{+/-}$ cells under conditions of metabolic stress or amino acid deprivation.

<u>Year 2:</u>

- Identifying increased K6 protein expression in autophagy-deficient immortalized mouse mammary epithelial cells and in tumors derived from these cells. The K6 protein however, was expressed only in a subset of cells.
- Identifying increased side-branching, ductal filling and proliferatin in *beclin1*$^{+/-}$ mammary glands.
- Identifying increased PR and RANKL signaling as the probable mechanism responsible for the increased proliferation and accelerated development observed in *beclin1*$^{+/-}$ mammary glands.
- Identifying the presence of increased amounts of cytokines such as IL-1β and TNF-α in developing *beclin1*$^{+/-}$ mammary glands, which could partly be responsible for the phenotype observed in these glands.

Reportable Outcomes:

Year1:

beclin1$^{+/+}$,Bcl-2 and *beclin1*$^{+/-}$, Bcl-2 immortalized mouse mammary epithelial cell lines stably overexpressing human WT K8, K8 S73A and K8 S73D constructs were generated for the purpose of this study.

Year 2:

A review article titled "The interplay between autophagy and ROS in tumorigenesis" was published in Frontiers Oncology with the help of this grant support.

Conclusions:

Year 1:

We were unable to make a valid conclusion from our examination of the differences in soluble and insoluble keratin fractions of *beclin1*$^{+/+}$ and *beclin1*$^{+/-}$ cell lines overexpressing Bcl-2 since usual methods of normalization are not useful in our case. Typically, the insoluble fraction is normalized by examining the keratin levels; however, we are interested in comparing the keratin levels and therefore, this is not a good control for our purposes. Additionally, the soluble fraction is generally normalized to the cell number, which again is not helpful in our case, since alterations in the levels of autophagy impact the overall protein level of the cells and therefore, autophagy-competent and deficient cells might have varying levels of overall protein.

Overexpression of WT K8, K8 S73A and K8 S73D constructs does not disrupt the keratin network or affect the levels of Phospho(S73)-K8 in *beclin1*$^{+/+}$ and *beclin1*$^{+/-}$ cell lines, overexpressing Bcl-2. Additionally, this overexpression does not affect viability under conditions of metabolic stress or amino acid deprivation. However, high levels of Phospho(S73)-K8 is associated with low levels of distant metastasis from Tumor Microarray staining. We are investigating if autophagy status of tumors affects their metastatic potential, since low beclin1 levels correlate with high Phospho(S73)-K8 levels, which in turn correlate with low levels of distant metastases.

High mRNA expression of K6, a marker of bipotent progenitor cells and a protein whose expression is associated with a wound healing response in injured cells, was detected in *beclin1*$^{+/-}$ cell lines, allograft tumors generated from these cell lines as well as mammary gland tissue of *beclin1*$^{+/-}$ mice, compared to their wild-type counterparts. We are currently testing if K6 expression is responsible for the higher tumorigenic potential of autophagy-deficient cell lines, when compared to the autophagy-competent ones. Identifying the proteins responsible for the tumorigenecity of autophagy-compromised cell lines will enable the development of drugs that target these proteins and will aid in the treatment of a particular subset of human breast tumors.

Year 2:

We were unable to knockdown the levels of K6 in *beclin1*$^{+/+}$ and *beclin1*$^{+/-}$ iMMECs overexpressing Bcl-2 since its expression is sporadic in a given population of cells. Moreover, the fact that K6 expression can be both constitutive and inducible depending upon external stimuli/stress (for example, wounding) makes this task challenging.

Since K6 expression is highest during pubertal mammary gland development, we examined whole mounts of mammary glands from *beclin1*$^{+/+}$ and *beclin1*$^{+/-}$, which revealed that the autophagy-deficient glands had increased side-branching and ductal filling. As signaling via progesterone receptor (PR) is responsible for side-branching in

the mammary gland, we examined the levels of PR in mammary glands from *beclin1*$^{+/+}$ and *beclin1*$^{+/-}$ mice. We observed higher levels of PR and the proliferative marker Ki67, in *beclin1*$^{+/-}$ glands indicating that these glands had higher levels of proliferation possibly due to increased PR signaling compared to wild-type glands. Furthermore, we observed higher levels of RANKL, which functions downstream of PR in mediating the proliferative effects of progesterone, in *beclin1*$^{+/-}$ mammary glands. We are currently in the process of investigating whether the increased levels of PR and RANKL signaling observed in the *beclin1*$^{+/-}$ glands are responsible for the increased hyperplasia observed in *beclin1*$^{+/-}$ glands by treating *beclin1*$^{+/+}$ and *beclin1*$^{+/-}$ mice with the carcinogen, DMBA.

In the developing mammary gland of 5-week old *beclin1*$^{+/-}$ mice, we observe increased levels of cytokines such as IL-1β and TNF-α in the stroma compared to wild-type glands. Importantly, earlier studies have demonstrated increased cytokine secretion in autophagy-impaired cells, which has been attributed to the high levels of ROS and increased inflammasome activity in these cells. We are currently testing if treating mice with antioxidants reduces the levels of cytokines, and in turn alleviates the increased side-branching, ductal filling, proliferation and hyperplasia observed in *beclin1*$^{+/-}$ mammary glands.

References:

Brisken, C., and O'Malley, B. (2010). Hormone action in the mammary gland. Cold Spring Harb Perspect Biol *2*, a003178.

Bu, W., Chen, J., Morrison, G.D., Huang, S., Creighton, C.J., Huang, J., Chamness, G.C., Hilsenbeck, S.G., Roop, D.R., Leavitt, A.D*., et al.* (2011). Keratin 6a marks mammary bipotential progenitor cells that can give rise to a unique tumor model resembling human normal-like breast cancer. Oncogene *30*, 4399-4409.

Fernandez-Valdivia, R., Mukherjee, A., Ying, Y., Li, J., Paquet, M., DeMayo, F.J., and Lydon, J.P. (2009). The RANKL signaling axis is sufficient to elicit ductal side-branching and alveologenesis in the mammary gland of the virgin mouse. Dev Biol *328*, 127-139.

Gonzalez-Suarez, E., Jacob, A.P., Jones, J., Miller, R., Roudier-Meyer, M.P., Erwert, R., Pinkas, J., Branstetter, D., and Dougall, W.C. (2010). RANK ligand mediates progestin-induced mammary epithelial proliferation and carcinogenesis. Nature *468*, 103-107.

Gross, O., Thomas, C.J., Guarda, G., and Tschopp, J. (2011). The inflammasome: an integrated view. Immunol Rev *243*, 136-151.

Karantza-Wadsworth, V., Patel, S., Kravchuk, O., Chen, G., Mathew, R., Jin, S., and White, E. (2007). Autophagy mitigates metabolic stress and genome damage in mammary tumorigenesis. Genes Dev *21*, 1621-1635.

Kongara, S., Kravchuk, O., Teplova, I., Lozy, F., Schulte, J., Moore, D., Barnard, N., Neumann, C.A., White, E., and Karantza, V. (2010). Autophagy regulates keratin 8 homeostasis in mammary epithelial cells and in breast tumors. Mol Cancer Res *8*, 873-884.

Ku, N.O., Azhar, S., and Omary, M.B. (2002). Keratin 8 phosphorylation by p38 kinase regulates cellular keratin filament reorganization: modulation by a keratin 1-like disease causing mutation. J Biol Chem *277*, 10775-10782.

Li, Y., Welm, B., Podsypanina, K., Huang, S., Chamorro, M., Zhang, X., Rowlands, T., Egeblad, M., Cowin, P., Werb, Z*., et al.* (2003). Evidence that transgenes encoding components of the Wnt signaling pathway preferentially induce mammary cancers from progenitor cells. Proc Natl Acad Sci U S A *100*, 15853-15858.

Liao, J., Ku, N.O., and Omary, M.B. (1997). Stress, apoptosis, and mitosis induce phosphorylation of human keratin 8 at Ser-73 in tissues and cultured cells. J Biol Chem *272*, 17565-17573.

Martinon, F., Mayor, A., and Tschopp, J. (2009). The inflammasomes: guardians of the body. Annu Rev Immunol *27*, 229-265.

Nakahira, K., Haspel, J.A., Rathinam, V.A., Lee, S.J., Dolinay, T., Lam, H.C., Englert, J.A., Rabinovitch, M., Cernadas, M., Kim, H.P., *et al.* (2011). Autophagy proteins regulate innate immune responses by inhibiting the release of mitochondrial DNA mediated by the NALP3 inflammasome. Nat Immunol *12*, 222-230.

Parmar, H., and Cunha, G.R. (2004). Epithelial-stromal interactions in the mouse and human mammary gland in vivo. Endocr Relat Cancer *11*, 437-458.

Saitoh, T., Fujita, N., Jang, M.H., Uematsu, S., Yang, B.G., Satoh, T., Omori, H., Noda, T., Yamamoto, N., Komatsu, M., *et al.* (2008). Loss of the autophagy protein Atg16L1 enhances endotoxin-induced IL-1beta production. Nature *456*, 264-268.

Sapino, A., Macri, L., Gugliotta, P., Pacchioni, D., Liu, Y.J., Medina, D., and Bussolati, G. (1993). Immunophenotypic properties and estrogen dependency of budding cell structures in the developing mouse mammary gland. Differentiation *55*, 13-18.

Schramek, D., Leibbrandt, A., Sigl, V., Kenner, L., Pospisilik, J.A., Lee, H.J., Hanada, R., Joshi, P.A., Aliprantis, A., Glimcher, L., *et al.* (2010). Osteoclast differentiation factor RANKL controls development of progestin-driven mammary cancer. Nature *468*, 98-102.

Smith, G.H., Mehrel, T., and Roop, D.R. (1990). Differential keratin gene expression in developing, differentiating, preneoplastic, and neoplastic mouse mammary epithelium. Cell Growth Differ *1*, 161-170.

Stingl, J. (2011). Estrogen and progesterone in normal mammary gland development and in cancer. Horm Cancer *2*, 85-90.

Toivola, D.M., Zhou, Q., English, L.S., and Omary, M.B. (2002). Type II keratins are phosphorylated on a unique motif during stress and mitosis in tissues and cultured cells. Mol Biol Cell *13*, 1857-1870.

Wojcik, S.M., Longley, M.A., and Roop, D.R. (2001). Discovery of a novel murine keratin 6 (K6) isoform explains the absence of hair and nail defects in mice deficient for K6a and K6b. J Cell Biol *154*, 619-630.

Zhou, R., Yazdi, A.S., Menu, P., and Tschopp, J. (2011). A role for mitochondria in NLRP3 inflammasome activation. Nature *469*, 221-225.

Appendix:

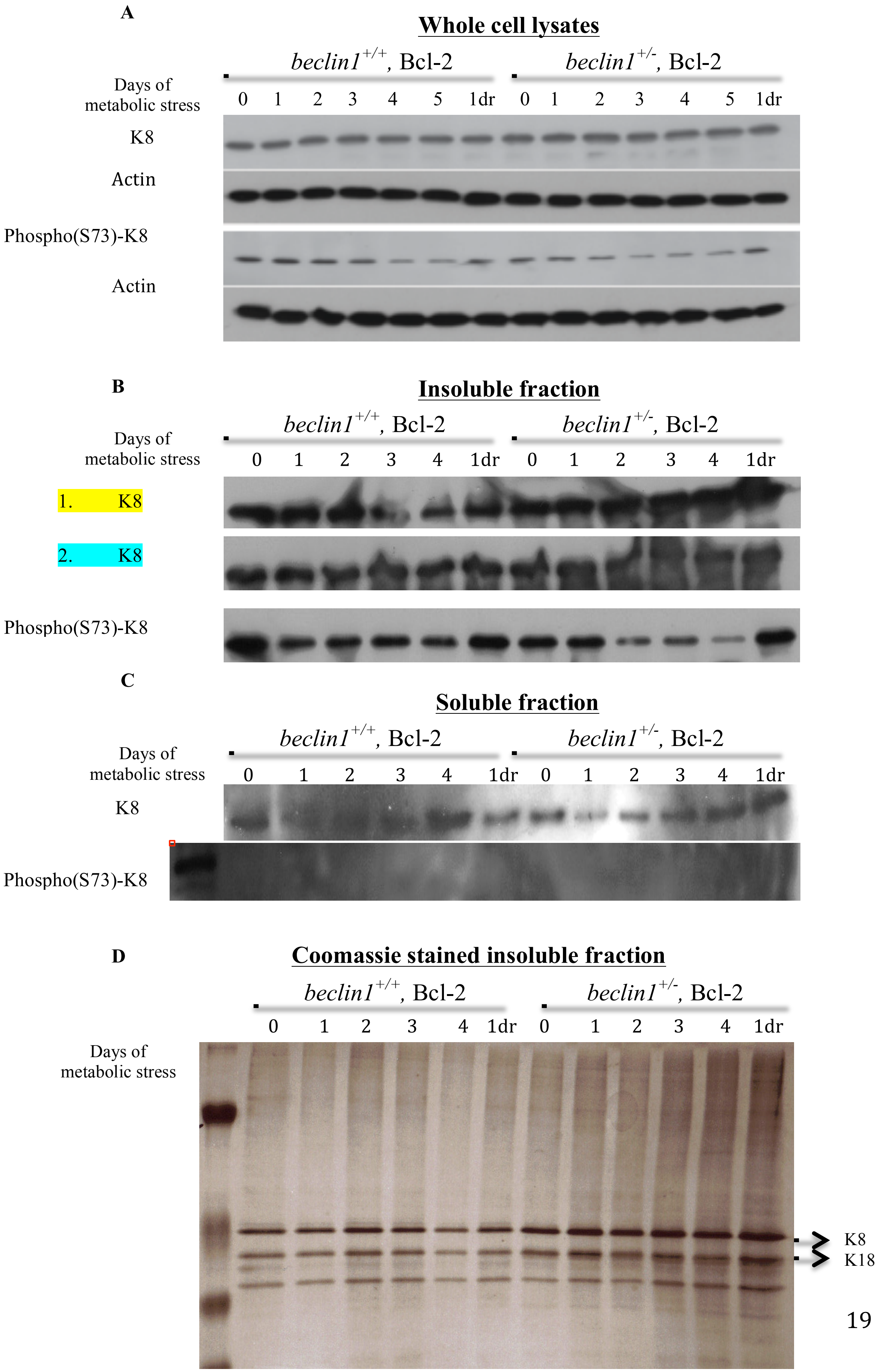
A
Whole cell lysates
beclin1+/+, Bcl-2
beclin1+/-, Bcl-2
Days of metabolic stress
0 1 2 3 4 5 1dr 0 1 2 3 4 5 1dr
K8
Actin
Phospho(S73)-K8
Actin
B
Insoluble fraction
beclin1+/+, Bcl-2
beclin1+/-, Bcl-2
Days of metabolic stress
0 1 2 3 4 1dr 0 1 2 3 4 1dr
1. K8
2. K8
Phospho(S73)-K8
C
Soluble fraction
beclin1+/+, Bcl-2
beclin1+/-, Bcl-2
Days of metabolic stress
0 1 2 3 4 1dr 0 1 2 3 4 1dr
K8
Phospho(S73)-K8
D
Coomassie stained insoluble fraction
beclin1+/+, Bcl-2
beclin1+/-, Bcl-2
0 1 2 3 4 1dr 0 1 2 3 4 1dr
Days of metabolic stress
K8
K18

<u>Figure 1</u>:

<u>1A</u> - Total cell lysates of *beclin1*$^{+/+}$ and *beclin1*$^{+/-}$ *cells* overexpressing Bcl-2 were subjected to metabolic stress (no glucose, low oxygen conditions) for 5 days and allowed to recover (normal nutrient and oxygen conditions) for 1 day and probed with antibodies recognizing K8 and Phospho(S73)-K8.

<u>1B</u> – Lysates of insoluble protein fractions isolated from *beclin1*$^{+/+}$ and *beclin1*$^{+/-}$ cells overexpressing Bcl-2 and metabolically stressed for 4 days and allowed to recover for 1 day were probed for levels of K8 and Phospho(S73)-K8. For the K8 blot (1. K8) highlighted in yellow, 20 μl of equal volume lysates was loaded, and for the K8 blot (2. K8) highlighted in turquoise, equal amount of protein was loaded on the basis of the BCA-RAC assay. The BCA-RAC assay was used to load equal amount of protein for the the Phospho(S73)-K8 blot.

<u>1C</u> – Lysates containing the triton-x soluble proteins were isolated from metabolically stressed (4 days, and 1 day recovery) *beclin1*$^{+/+}$ and *beclin1*$^{+/-}$ cells with Bcl-2 and probed for K8 and Phospho(S73)-K8 levels. Equal amounts of protein were loaded on the basis of the BCA-RAC assay. No Phospho(S73)-K8 was detected in the soluble fraction; the lane highlighted in red contains the lysate of the insoluble fraction of *beclin1*$^{+/+}$, Bcl-2 cell line, which serves as a positive control.

<u>1D</u> – Equal volume of lysates containing the insoluble protein component of metabolically stressed *beclin1*$^{+/+}$ and *beclin1*$^{+/-}$ cells were loaded onto a gel and stained with Coomassie Blue to detect keratins, which are the predominant components of insoluble extract.

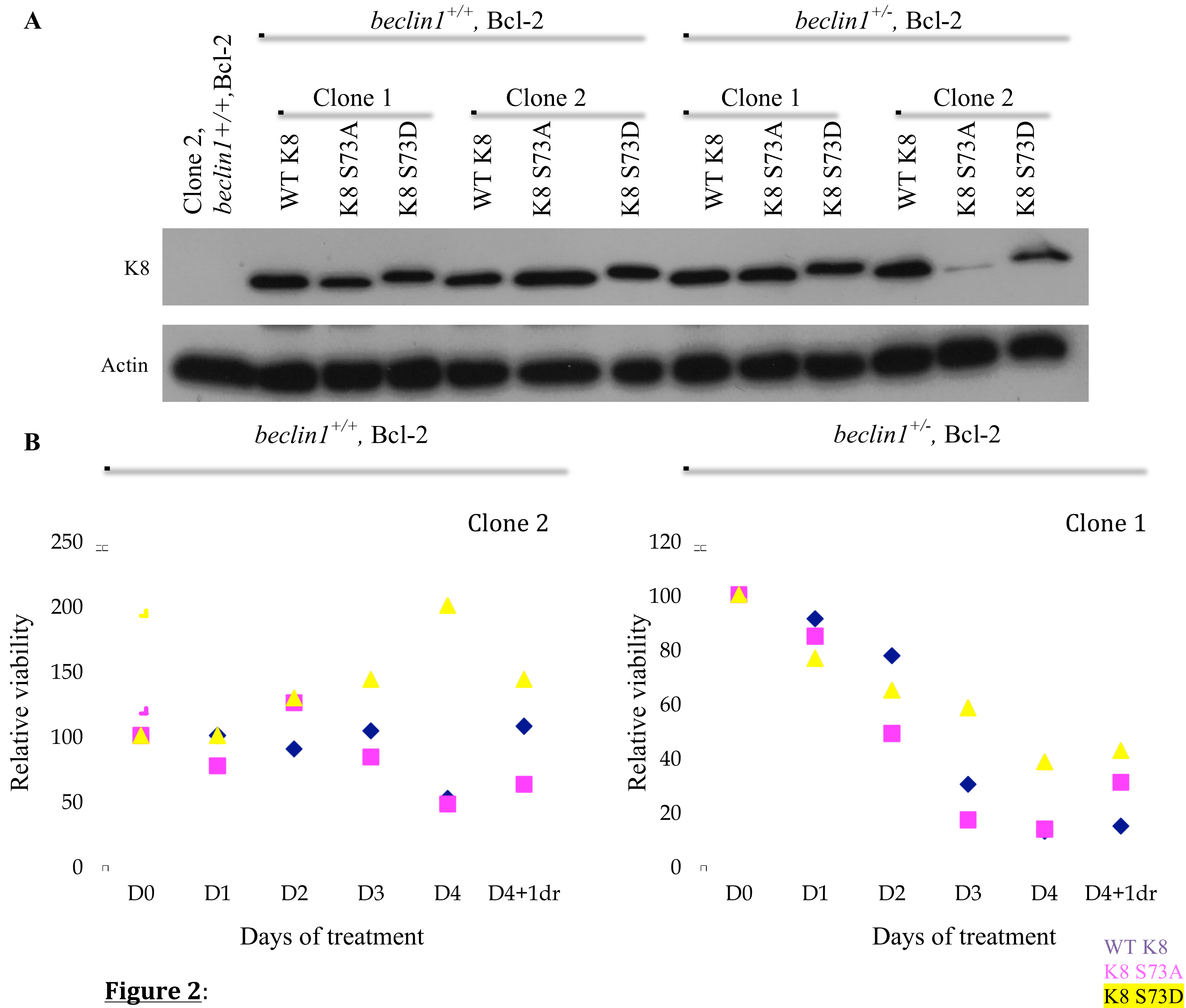

Figure 2:

2A – Western blot showing the overexpression of human WT K8, K8 S73A, and K8 S73D constructs in two *beclin1*$^{+/+}$. Bcl-2 and *beclin1*$^{+/-}$, Bcl-2 parental cell lines. The antibody used is specific to the human protein and does not detect any mouse protein (absence of band in the first lane, which contains the parental *beclin1*$^{+/+}$, Clone 2 lysate).

2B - Viability of *beclin1*$^{+/+}$, Bcl-2 and *beclin1*$^{+/-}$, Bcl-2 cells overexpressing WT K8 (blue line), K8 S73A (pink line) and K8 S73D (yellow line) constructs metabolic stress (no glucose, low oxygen conditions) for a duration of 0, 1, 2, 3, and 4 days (D0, D1, D2, D3, D4) and allowed to recover (restoration of normal glucose and oxygen conditions) for a day (D4+1Dr). Using cell lines derived from a single parental clone

of each genotype, it appears that the K8 S73D construct aids in the survival of both *beclin1*$^{+/+}$ and *beclin1*$^{+/-}$ cells overexpressing Bcl-2 under stress.

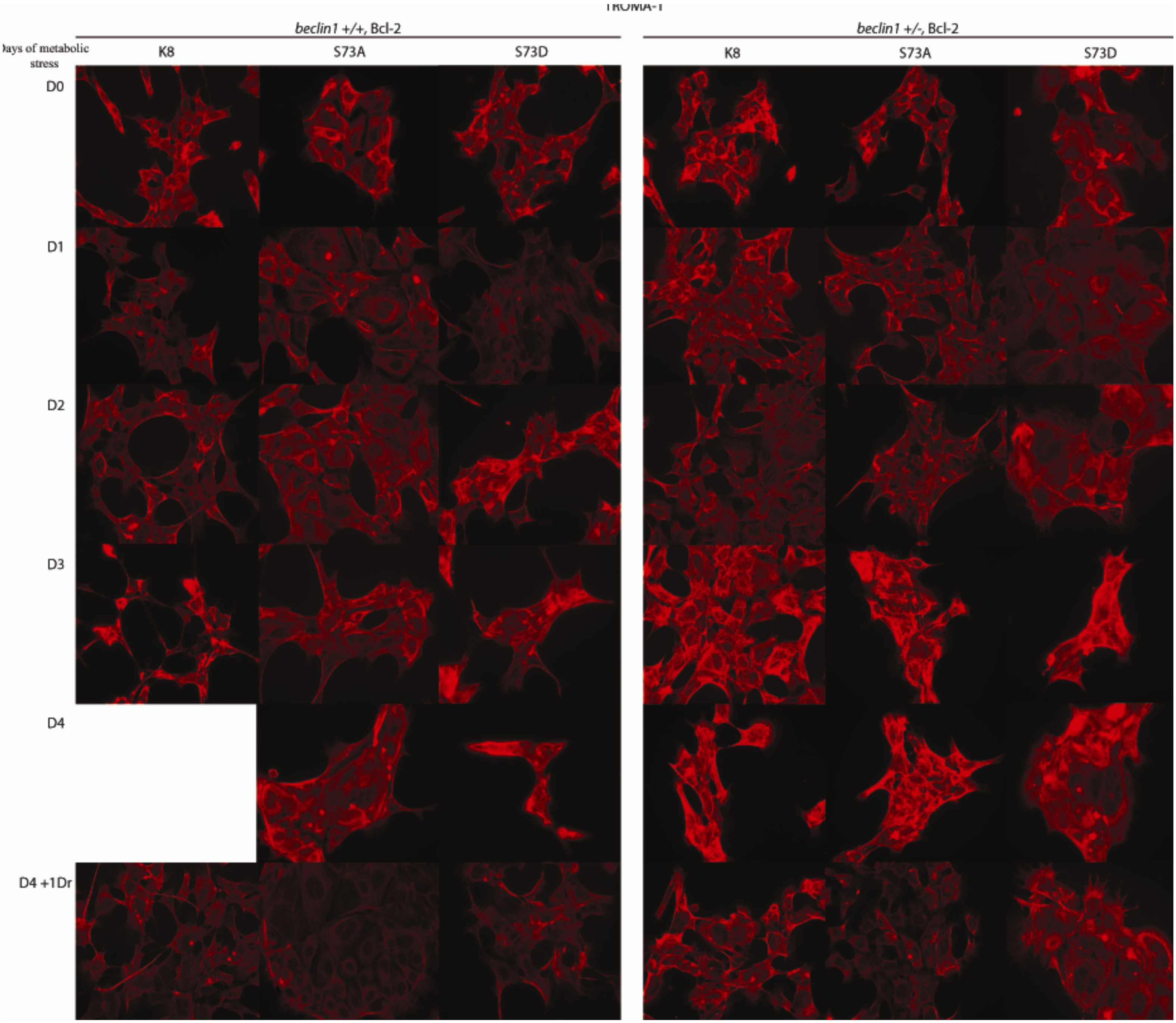

<u>Figure 3</u>: TROMA-1 (K8) expression and filament organization in *beclin1*$^{+/+}$, Bcl-2 and *beclin1*$^{+/-}$,Bcl-2 cells overexpressing WT K8, K8 S73A and K8 S73D constructs treated with metabolic stress for a period of 0, 1, 2, 3 and 4 days (D0, D1, D2, D3 and D4, respectively) and allowed to recover for a day (D4+1Dr). The heterozygous cells express higher levels of the protein compared to the wild-type cells in response to stress (day 3, 4 an
d during recovery); however, no differences in expression or filament structure are seen across the WT and mutant keratin constructs within and between each genotype. (Note: The slide containing the day 4 timepoint of the *beclin1*$^{+/+}$,Bcl-2 overexpressing WT K8 was damaged and could therefore, not be

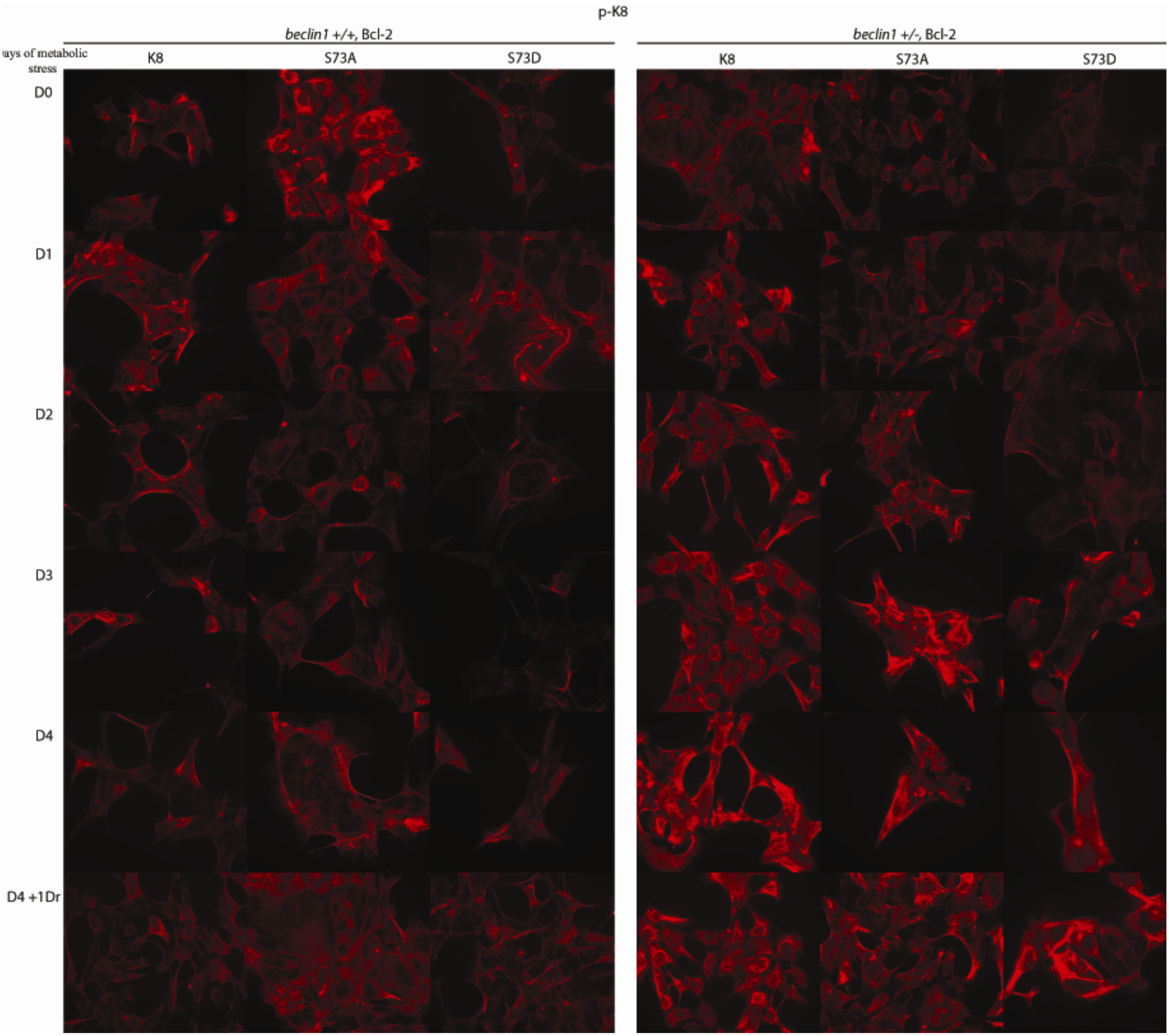

Figure 4: Phospho(S73)-K8 expression in *beclin1*$^{+/+}$, Bcl-2 and *beclin1*$^{+/-}$,Bcl-2 cells overexpressing WT K8, K8 S73A and K8 S73D constructs treated with metabolic stress for a period of 0, 1, 2, 3 and 4 days (D0, D1, D2, D3 and D4, respectively) and allowed to recover for a day (D4+1Dr). The heterozygous cells express higher levels of the protein compared to the wild-type cells on day 2, 3 and 4, and during recovery; however, no differences in expression are seen across the WT and mutant keratin constructs within and between each genotype.

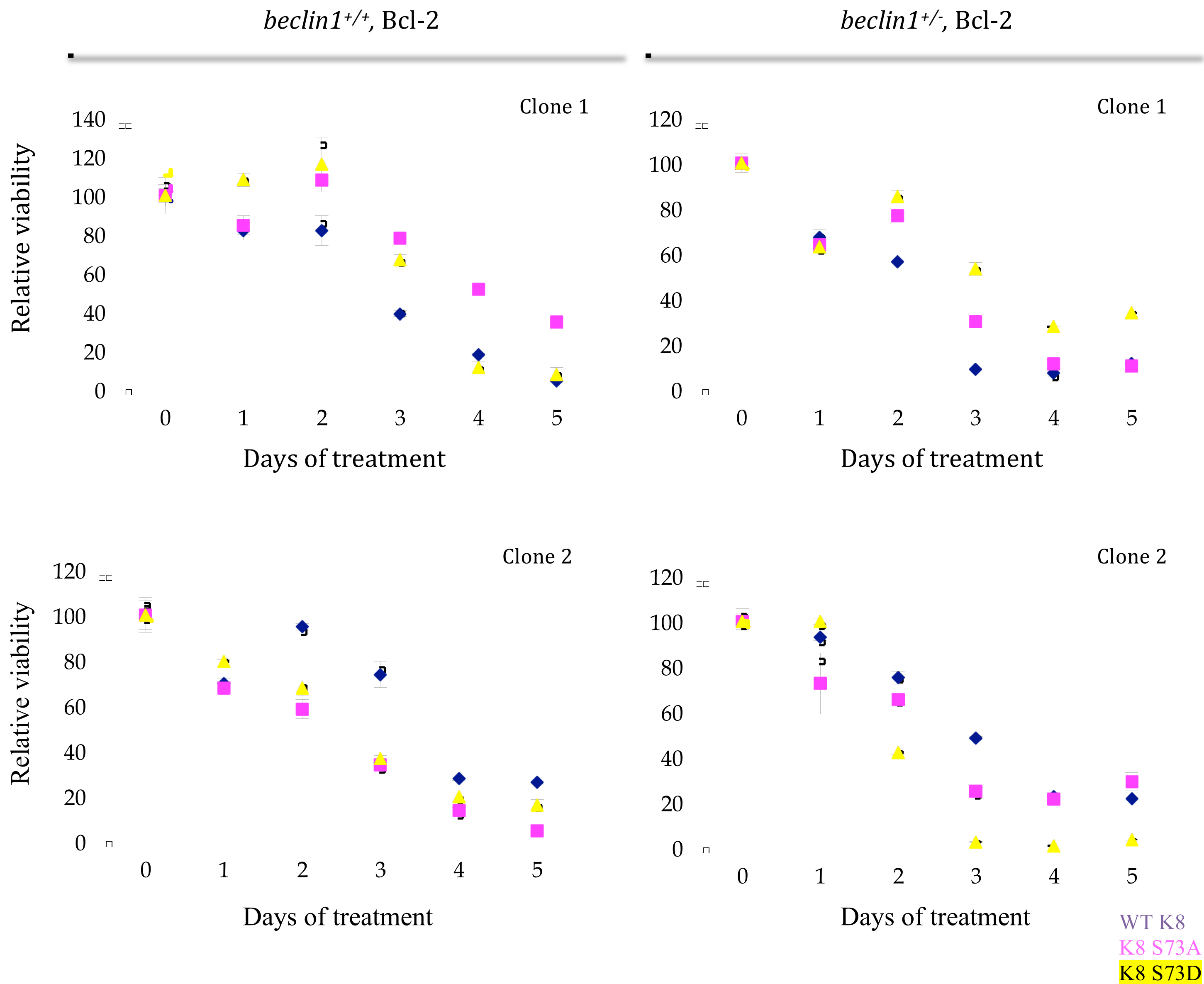

Figure 5: Viability of *beclin1*$^{+/+}$, Bcl-2 and *beclin1*$^{+/-}$, Bcl-2 cells overexpressing WT K8 (blue line), K8 S73A (pink line) and K8 S73D (yellow line) constructs (derived from two parental clones, Clone 1 and 2) under amino acid deprivation (Hanks buffered salt solution treatment) over a period of 5 days. No consistent pattern emerged from this assay.

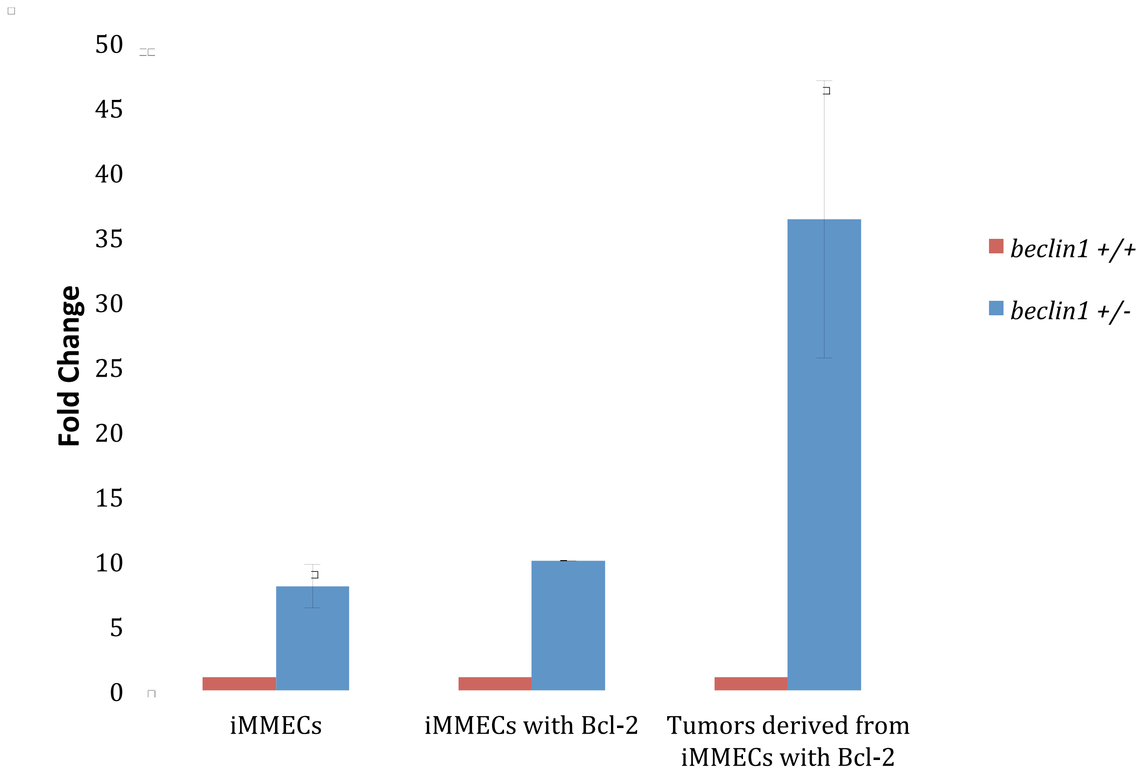

Figure 6: Gene expression profiling of *beclin1*$^{+/+}$ and *beclin1*$^{+/-}$ immortalized mouse mammary epithelial cells (iMMECs) with and without Bcl-2 and tumors generated from iMMECs with Bcl-2 indicates the presence of a higher Keratin 6 mRNA levels in the autophagy-deficient background compared to their wild-type counterparts.

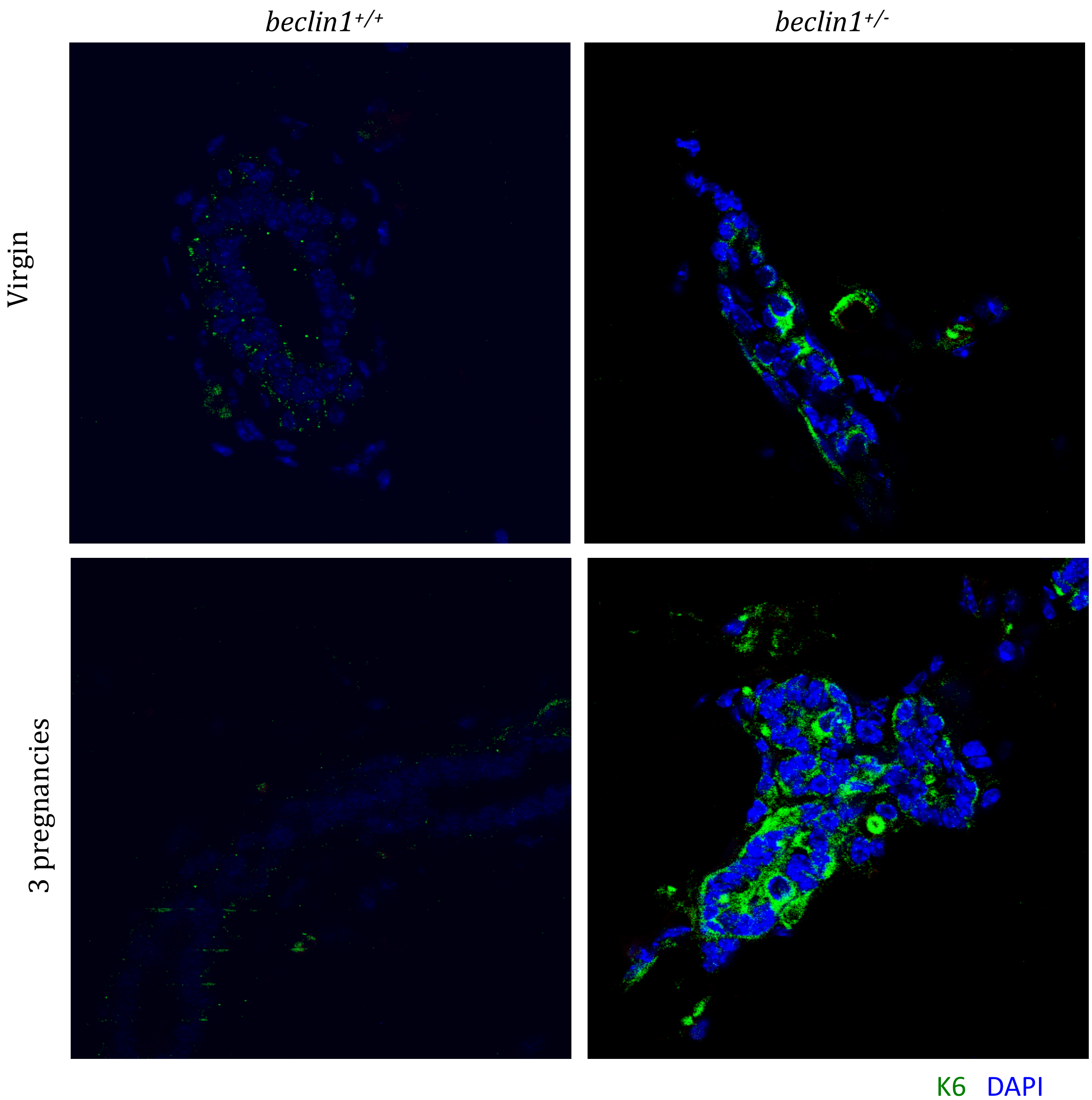

<u>Figure 7</u>: Mammary gland tissue from 11-month old *beclin1*$^{+/+}$ and *beclin1*$^{+/-}$ tissue was stained for Keratin 6 (in green) and DAPI (in blue). The *beclin1*$^{+/-}$ tissues express higher levels of Keratin 6 irrespective of the number of pregnancy cycles of the gland.

beclin1$^{+/+}$ *beclin1$^{+/-}$*

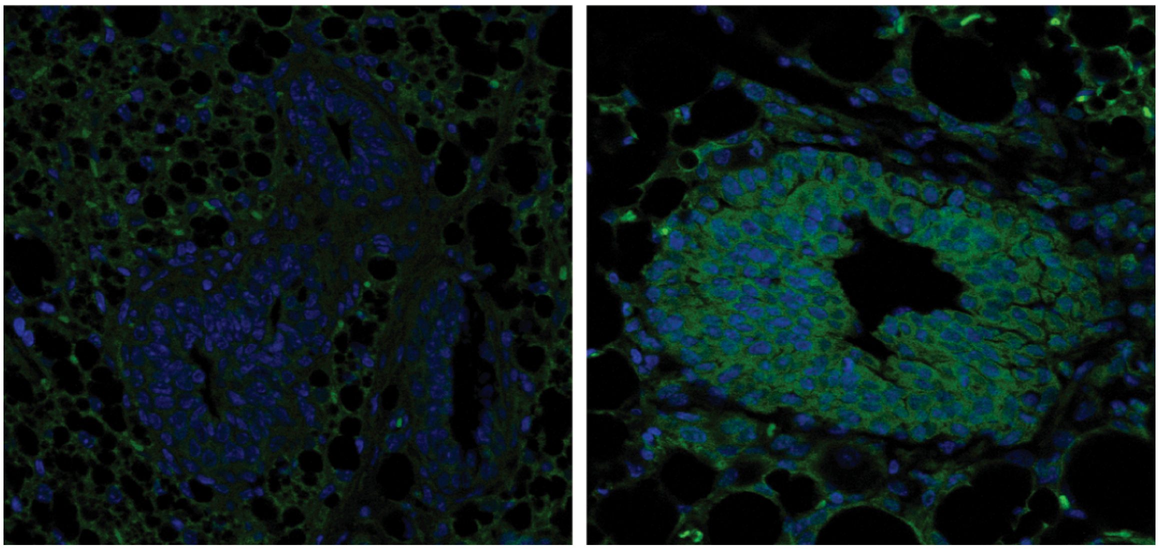

K6 DAPI

<u>Figure 8</u>: Mammary gland tissue from 4.5-week old *beclin1$^{+/+}$* and *beclin1$^{+/-}$* mice demonstrates higher levels of Keratin 6 in the autophagy-compromised tissue compared to the autophagy competent one.

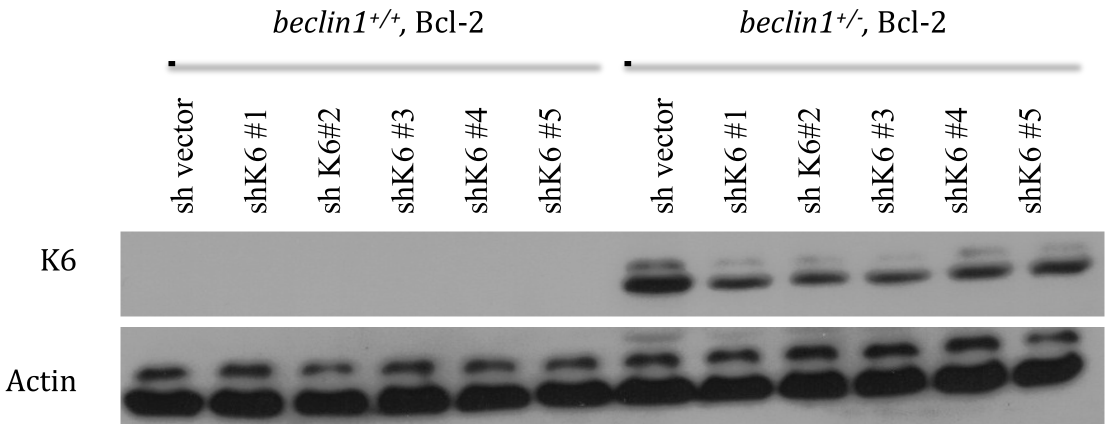

<u>Figure 9</u>: *beclin1$^{+/+}$* and *beclin1$^{+/-}$* iMMECs overexpressing Bcl-2 were transiently transfected with various shRNA constructs targeting K6 (shK6 #1 -#5) or a non-targeting vector control (sh vector) to test the efficacy of knockdown. The K6 blot above shows that sh K6 constructs #2 and #3 had the best knockdown. These constructs were used to conduct subsequent studies.

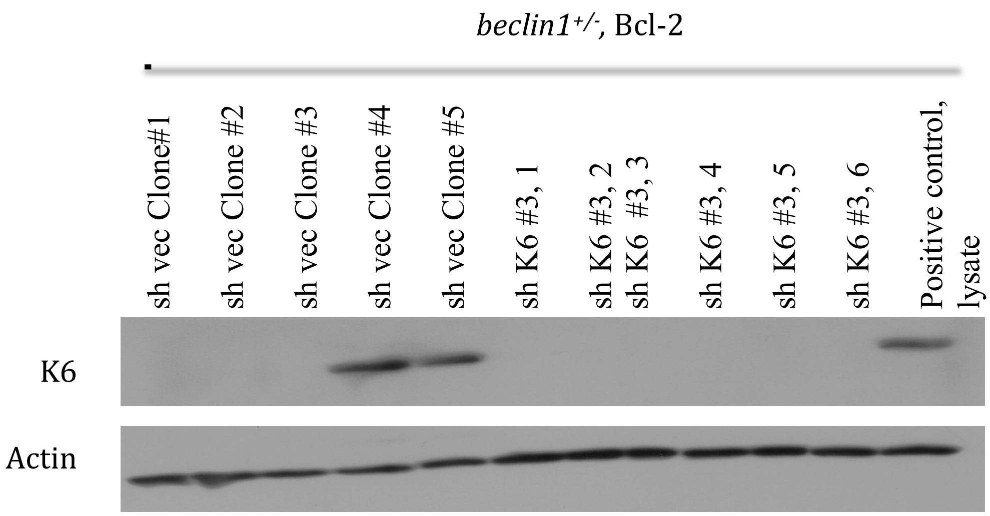

<u>**Figure 10**</u>: shRNA constructs targeting K6 (shK6 #2 and #3) or a non-targeting vector control (sh vector) were introduced into *beclin1*$^{+/+}$ and *beclin1*$^{+/-}$ iMMECs overexpressing Bcl-2 by lentiviral infection. Following infection, resistant colonies were allowed to emerge and independent colonies were picked. The blot here contains lysates of *beclin1*$^{+/-}$, Bcl-2 cells that stably expressed the vector control (sh vec, Clone #1-#5) or shRNA targeting K6 (sh K6, 1-6). Unexpectedly, we observed a heterogenous expression of K6 in the vector controls. Clones #1-3 have no detectable levels of K6, while Clones #4 and #5 have robust K6 expression. This result indicated not all cells within the parental *beclin1*$^{+/-}$, Bcl-2 cell line expresses K6.

K6 and DAPI

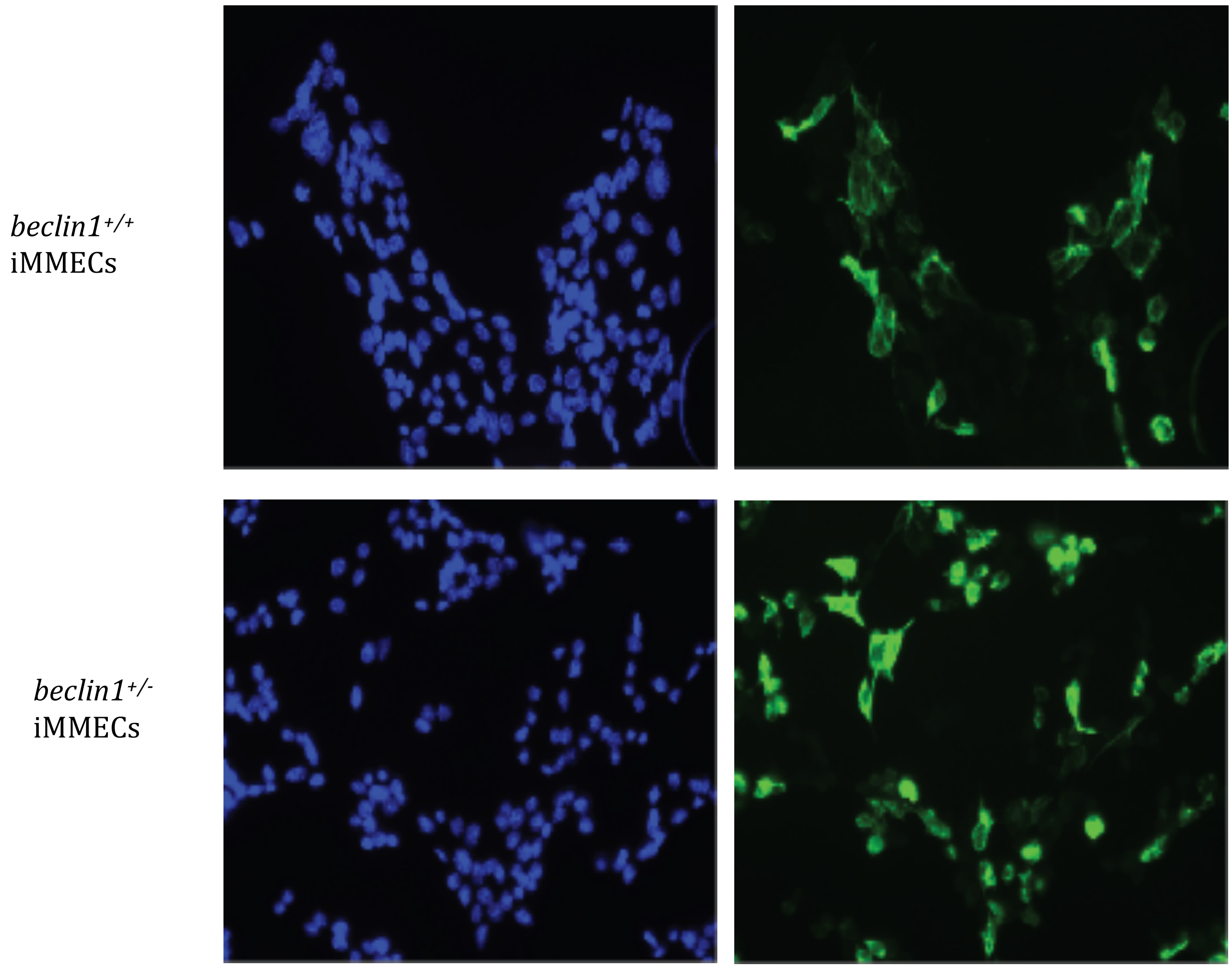

Figure 11: Immunofluorescence on *beclin1*$^{+/+}$ and *beclin1*$^{+/-}$ iMMECs revealed that while beclin1+/- cells did indeed have higher levels of K6 expression, not all cells within a cell line demonstrated K6 positivity.

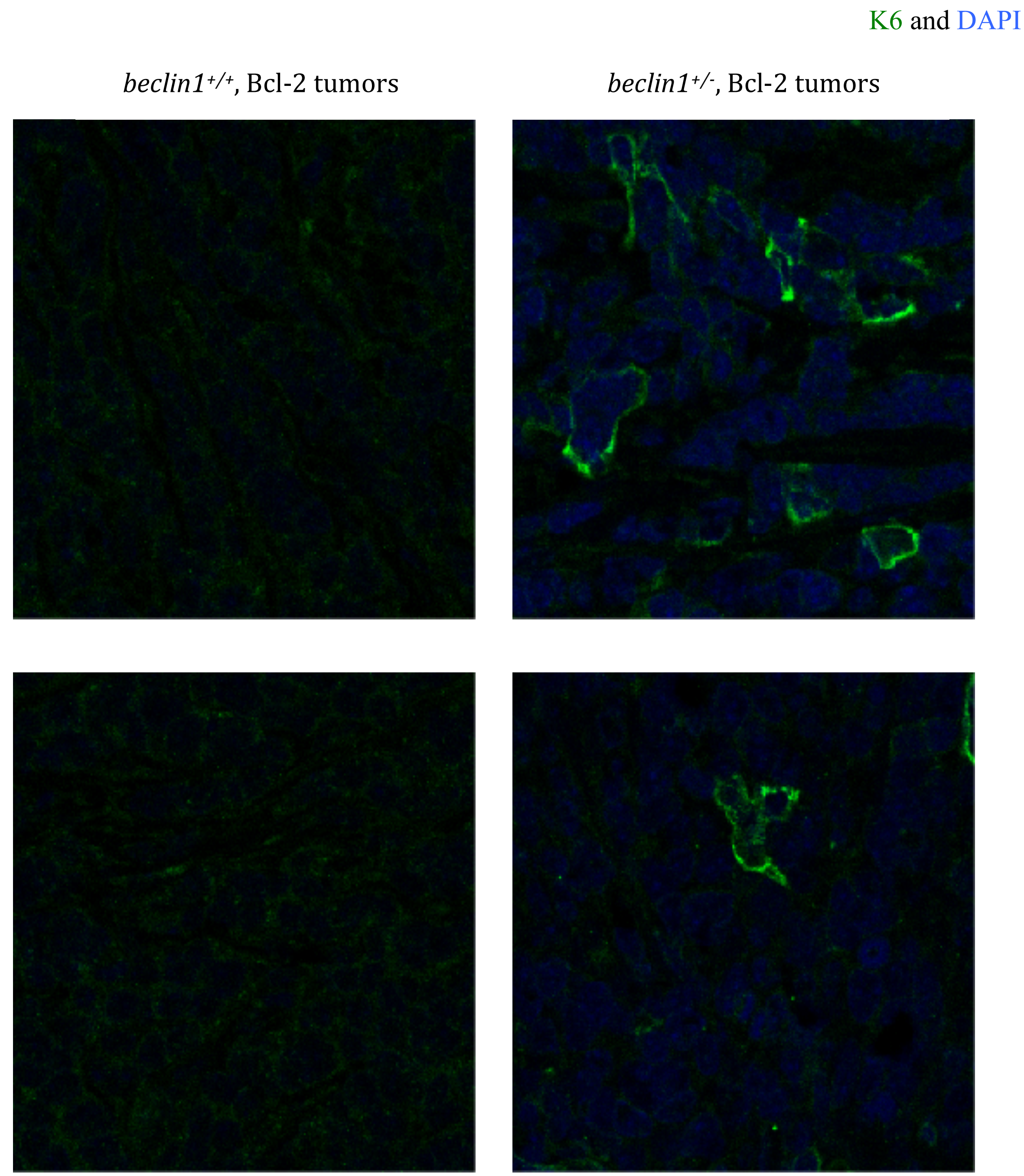

Figure 12: Tumors generated from orthotopic implantation of *beclin1*$^{+/+}$,Bcl-2 and *beclin1*$^{+/-}$,Bcl-2 iMMECs demonstrate higher levels of Keratin 6 in the autophagy-compromised background compared to the autophagy competent one.

K6 and DAPI

HCC1937 HCC1954

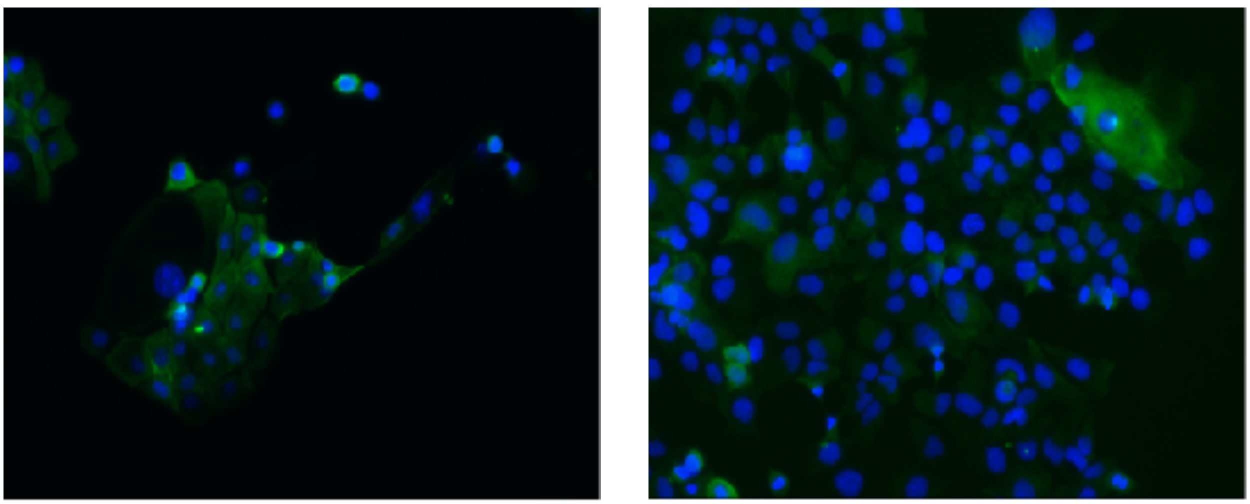

<u>Figure 13</u>: Human breast cancer cell lines HCC1937 and HCC1954, which have low beclin1 mRNA levels relative to a panel of human breast cancer cell lines, were stained for K6 by immunofluorescence. Similar to the iMMECs, the human breast cancer cell lines express K6 sporadically.

beclin1$^{+/+}$ *beclin1*$^{+/-}$

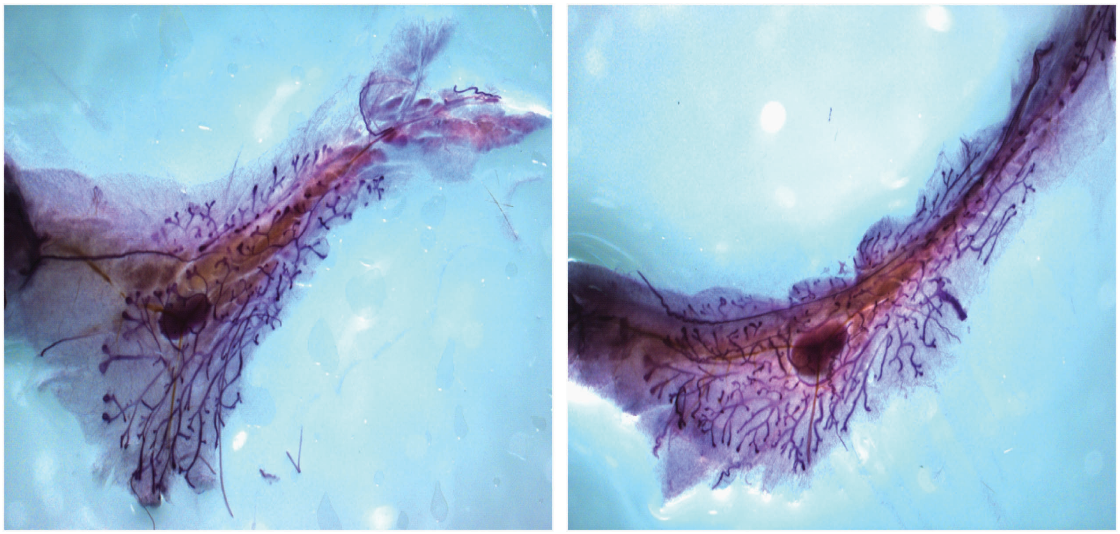

<u>Figure 14:</u> Whole mounts prepared from the native mammary glands of 6.5-week old *beclin1*$^{+/+}$ and *beclin1*$^{+/-}$ mice show increased side-branching and ductal filling in *beclin1*$^{+/-}$ mice.

Ki67
5-week old glands

beclin1$^{+/+}$ *beclin1*$^{+/-}$

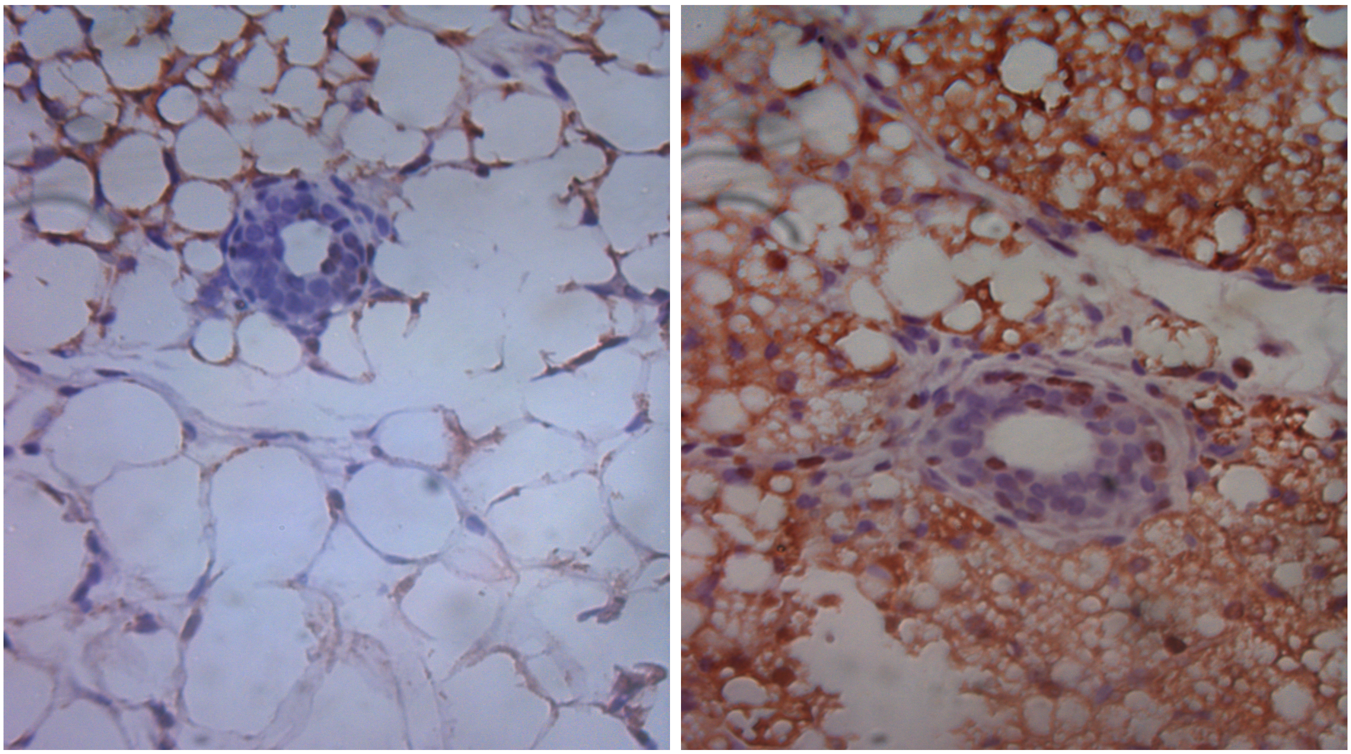

Figure 15: Mammary glands from 5-week old *beclin1*$^{+/-}$ mice exhibit increased levels of the proliferation marker, **Ki67.**

PR and K6
5-week old glands

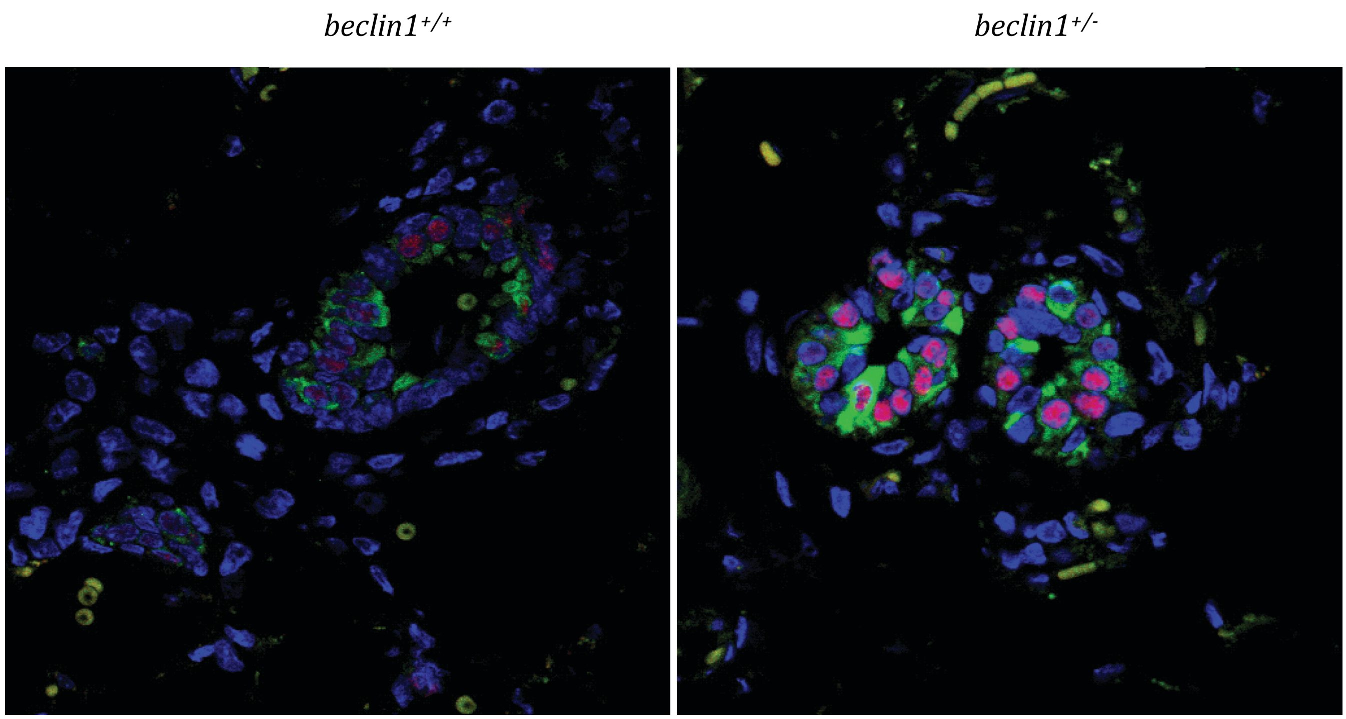

<u>Figure 16</u>: Mammary glands from 5-week old *beclin1*$^{+/-}$ mice exhibit increased levels of K6 and progesterone receptor (PR).

RANKL
DAPI
5-week old glands

beclin1$^{+/+}$ *beclin1*$^{+/-}$

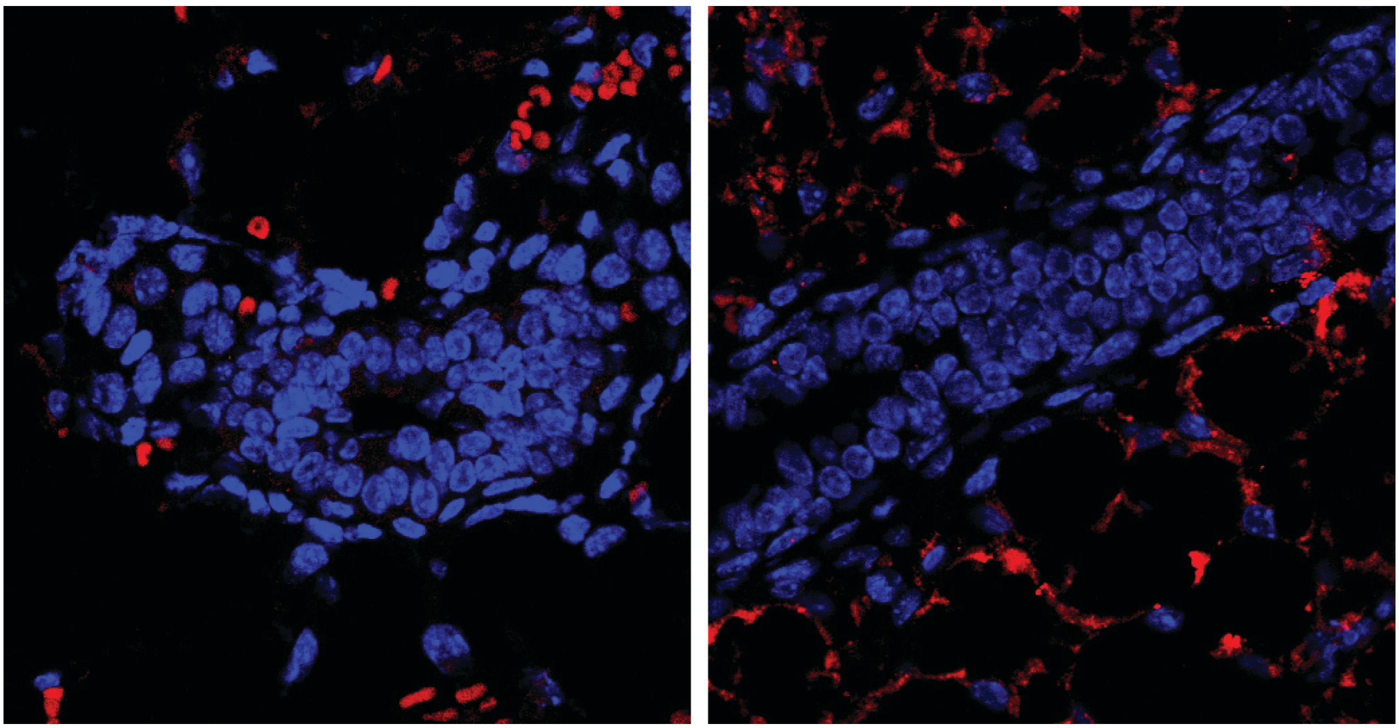

Figure 17: Native mammary glands from 5-week old *beclin1*$^{+/-}$ mice exhibit increased levels of RANKL, which localizes to the stroma.

PR
6.5-week old glands

beclin1$^{+/+}$ *beclin1$^{+/-}$*

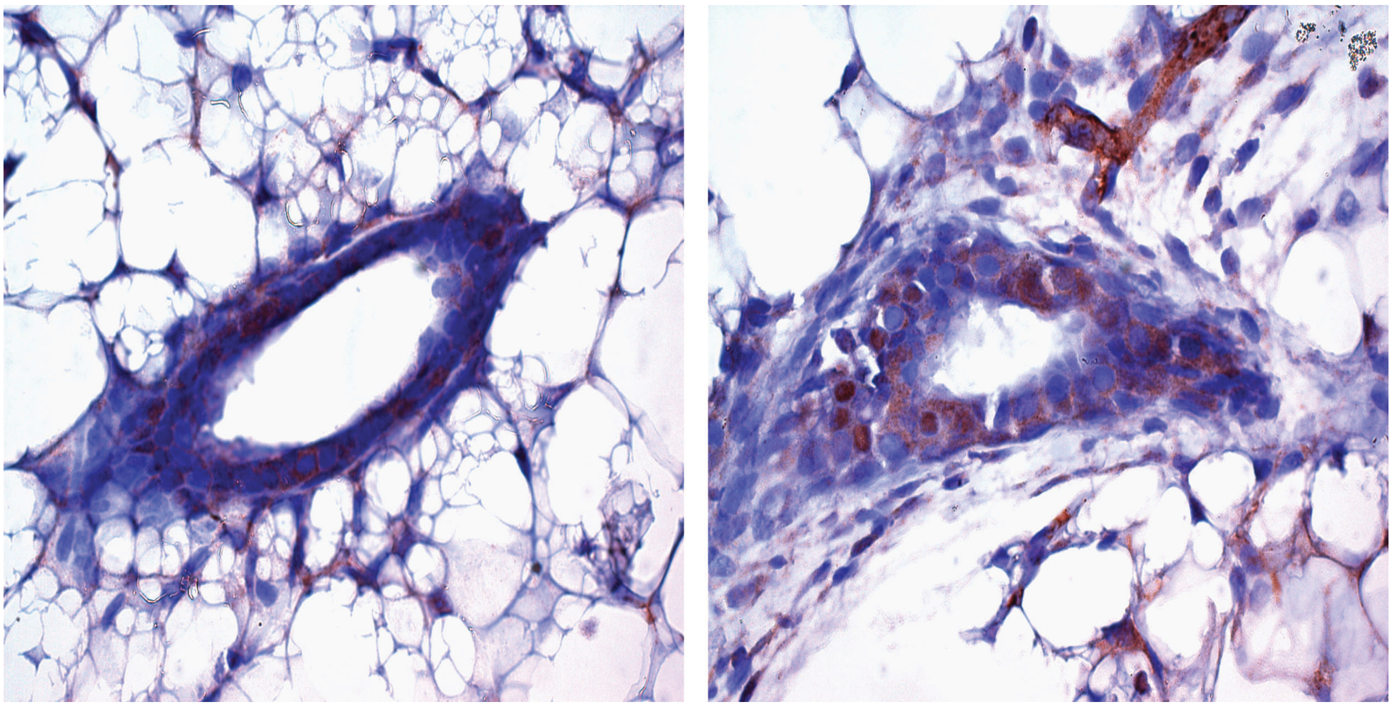

<u>Figure 18</u>: Mammary glands from 6.5-week old *beclin1$^{+/-}$* mice exhibit increased levels of **nuclear PR**.

RANKL
DAPI
6.5-week old glands

beclin1$^{+/+}$ *beclin1*$^{+/-}$

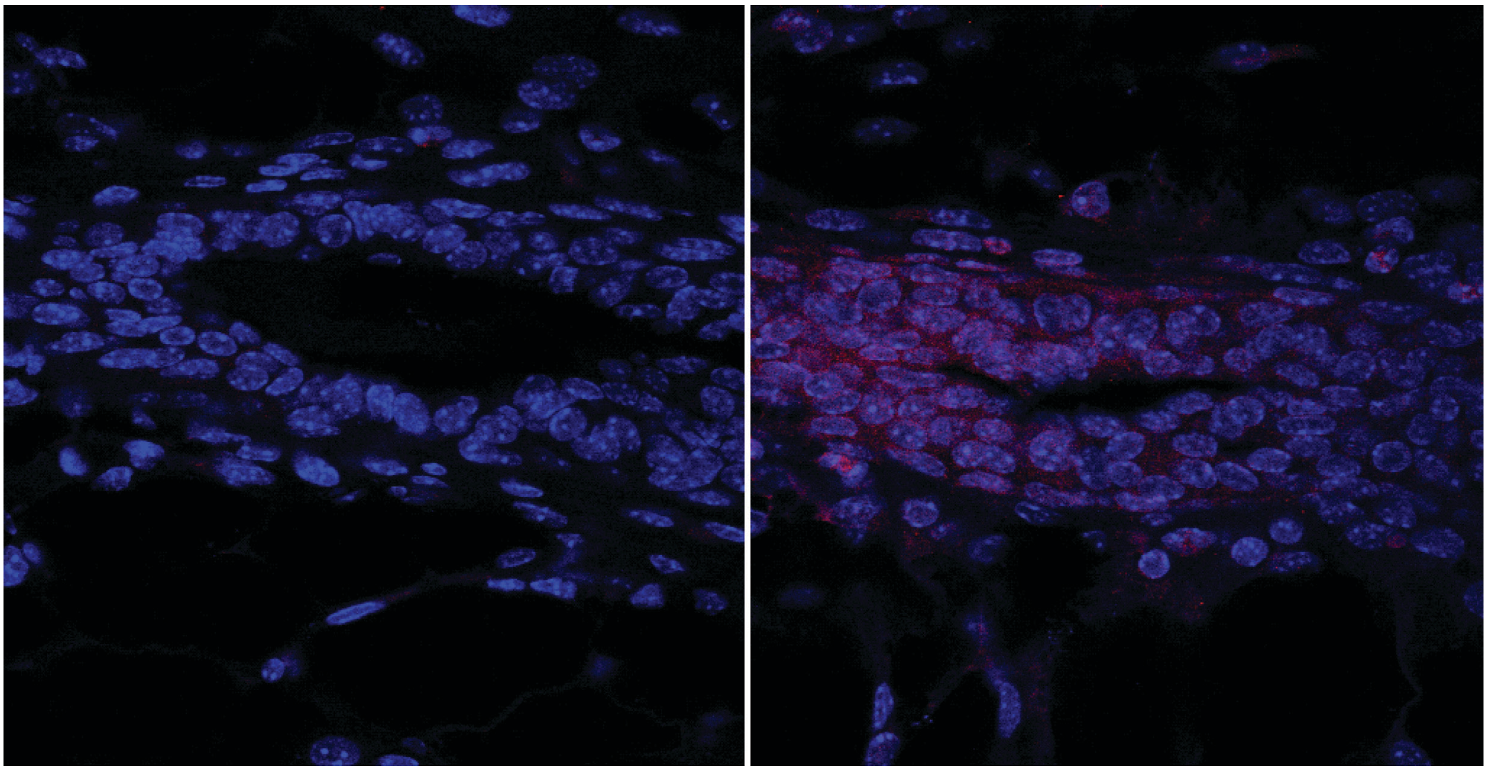

Figure 19: Mammary glands from 6.5-week old *beclin1*$^{+/-}$ mice exhibit increased levels of RANKL, which appears to be confined to the epithelial cells at this age.

TNF-α
5-week old glands

beclin1$^{+/+}$ *beclin1*$^{+/-}$

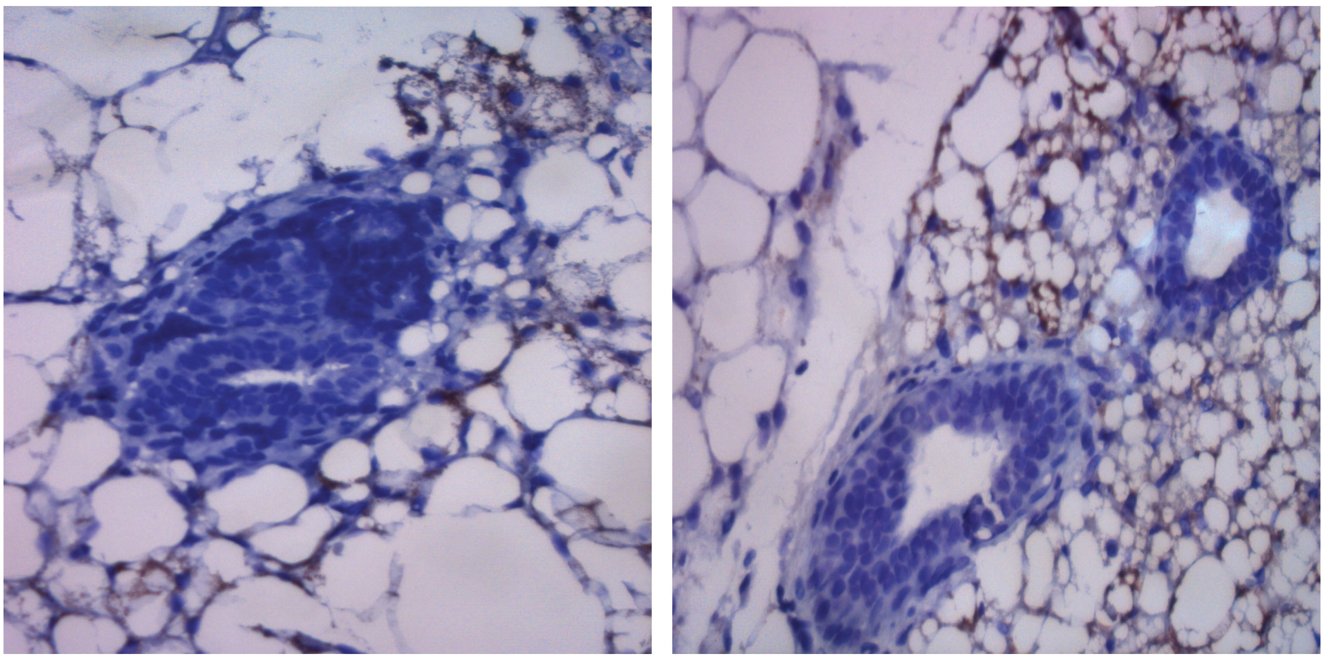

Figure 20: Increased level of **TNF-α** is observed in the native mammary glands of 5-week old *beclin1*$^{+/-}$ mice compared to their wild-type counterparts. Interestingly, this cytokine is predominantly detected in the stroma.

IL-1β
5-week old glands

beclin1$^{+/+}$ *beclin1*$^{+/-}$

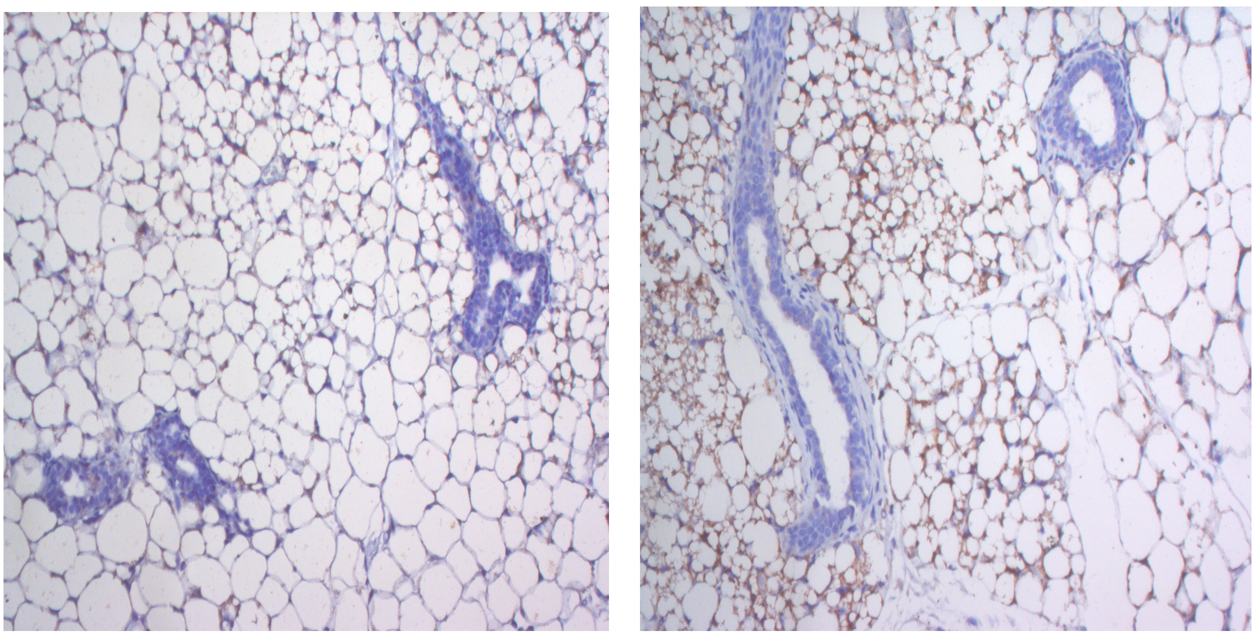

<u>Figure 21</u>: Native mammary glands from 5-week old *beclin1*$^{+/-}$ mice contain increased stromal levels of the cytokine **IL-1β.**

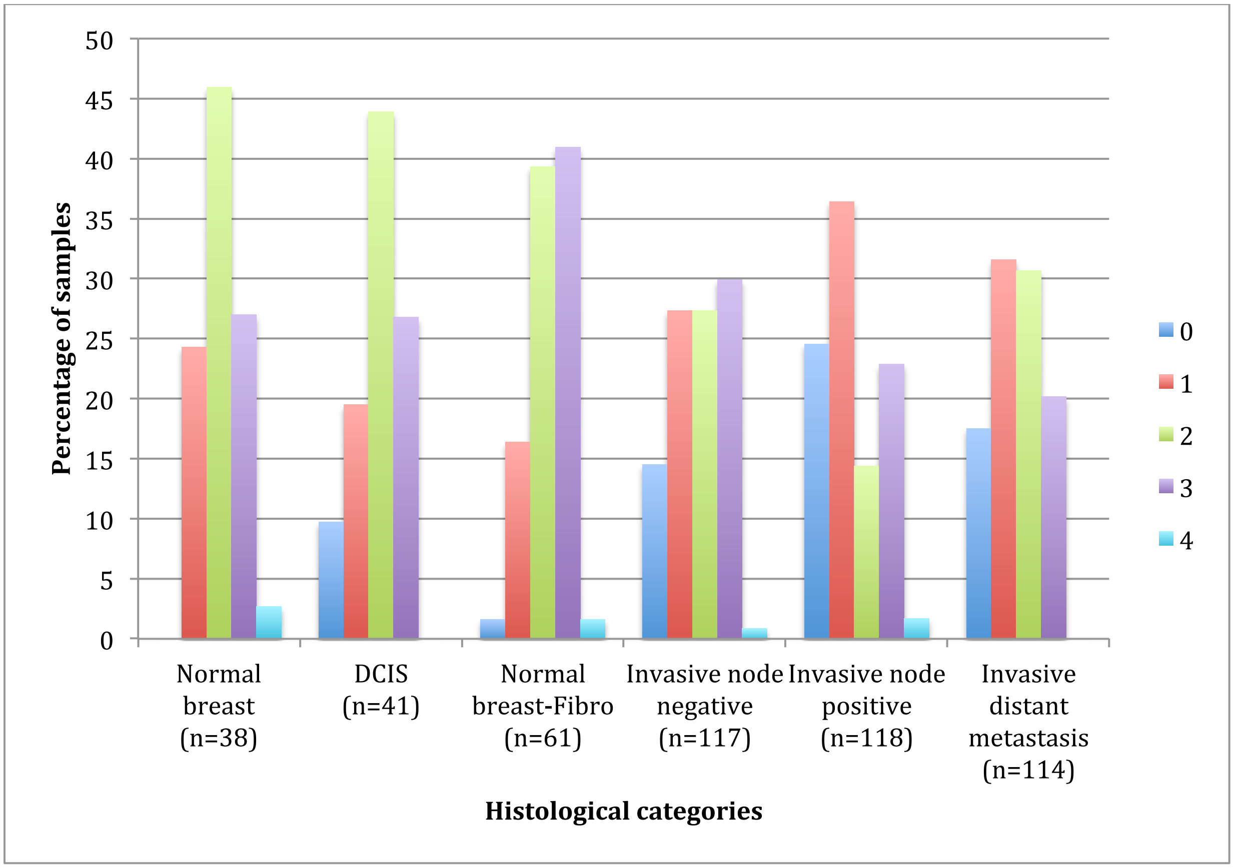

Figure 22: Human breast tumor microarray containing tissue from normal breast, DCIS, normal breast-fibroadenoma, and breast tumor samples from patients with invasive disease (node negative, positive and distant metastasis) was stained with a Phospho(S73)-K8 antibody. Low levels (0-1 score) of Phospho(S73)-K8 are present mostly in invasive specimens (node negative 41.8%, node positive 60.9%, and distant metastasis 49%), while this phenomenon is not observed in the normal tissue (24.3% in normal, and 28.2% in normal breast-fibroadenoma), indicating that autophagy status might be an important determiner of the metastatic potential of cells.